B. TECH. PROJECT REPORT

On

Synthesis and Characterization of HEA reinforced Al composites

BY

Ashish Singhal

DISCIPLINE OF METALLURGICAL ENGINEERING AND MATERIAL SCIENCE

INDIAN INSTITUTE OF TECHNOLOGY INDORE

December 2019

Synthesis and Characterization of HEA reinforced Al composites

A PROJECT REPORT

Submitted in partial fulfillment of the
requirements for the award of the degrees

of
BACHELOR OF TECHNOLOGY
in

METALLURGICAL ENGINEERING AND MATERIAL SCIENCE

Submitted by:
Ashish Singhal

Guided by:
Dr. Vinod Kumar, Assistant Professor, IIT Indore

INDIAN INSTITUTE OF TECHNOLOGY INDORE
December 2019

CANDIDATE'S DECLARATION

We hereby declare that the project entitled **"Synthesis and Characterization of HEA reinforced Al composites"** submitted in partial fulfillment for the award of the degree of Bachelor of Technology in 'Metallurgical Engineering And Material Science' completed under the supervision of **Dr. Vinod Kumar. Assistant Professor,** IIT Indore is an authentic work.

Further, I/we declare that I/we have not submitted this work for the award of any other degree elsewhere.

Signature and name of the student(s) with date

CERTIFICATE by BTP Guide(s)

It is certified that the above statement made by the students is correct to the best of my/our knowledge.

Signature of BTP Guide(s) with dates and their designation

Preface

This report on “Synthesis and Characterization of HEA reinforced Al composites” is prepared under the guidance of Dr. Vinod Kumar.

The project contains comparison of surface and mechanical properties of Al Matrix composites reinforced with FeCrAlMnNi High Entropy Alloy synthesized by different processing routes. Composites were synthesized by different processing routes (High energy Ball milling) and Stir Casting.

The prepared composites were characterized using XRD, Optical microscope, and hardness was calculated. The report focuses on analysis of results observed.

Ashish Singhal
B.Tech. IV Year
Discipline of Metallurgical Engineering And Material Science
IIT Indore

Acknowledgements

I wish to thank **Dr. Vinod Kumar** for his kind support and valuable guidance. The whole of this work is carried out under his guidance. His wide research experience and expertise in the subject helped me in understanding scientific topics at a deeper level. I also thank them for his trust in me and for giving me a lot of freedom to try new ideas.

I would also like to thank **Dr. Parasharam Shirage** for providing departmental facilities for smooth conduct of research.

It is their help and support, due to which I became able to complete the design and technical report. Without their support this report would not have been possible.

I would also like to take this opportunity to thank my labmates from **Physical Metallurgy Lab** for their company and being supportive all the time. A special thanks to **Mr. Sheetal Kumar Dewangan** for their technical expertise and many discussions, which proved invaluable to the work in this thesis and also like to acknowledge their willingness to help, and especially with the setting up of experiments and their patience in answering all my questions.

Ashish Singhal
B.Tech. IV Year
Discipline of Metallurgy And Material Science
IIT Indore

Abstract

Aluminium Matrix composites were developed using 1% equiatomic FeCrAlMnNi high entropy particles as the reinforcement phase. High entropy alloy powder were prepared by mechanical alloying in high energy ball mill. FeCrAlMnNi high entropy alloy has shown predominant body centered cubic (BCC) phase after 20hrs of ball millng. Composite was formed using different processing routes which are stir casting method and High Energy Ball Milling. Microstructure and hardness analysis is done to compare Pure Al and Al-HEA composite specimens. In Stir Casting optical micrograph reveals that the BCC phase FeCrAlMnNi High Entropy Particles were accumulated connecting grain boundaries of face centered cube (FCC) phase aluminium particles. This change is attributed to increase in Hardness of as cast Al-1% HEA as compared to pure Al. Harder high entropy particles were binded strongly to aluminium grain boundaries. Further investigations on specimens are done to check uniform distribution of reinforcement particles to study the effect of cooling, sedimentation. No significant change is seen in microstructure in direction of heat flow (radially outwards) which confirms that cooling of ingot in mould has no effect on homogeneity of composite due to slow cooling of cast ingot. It is observed that the hardness is maximum at center of cast ingot compared to top and bottom portion of ingot. indicating that the higher concentration of binder particles is present at the center of ingot, which was possibly due to the pouring mechanism used in mould. As in the bottom part melt solidifies first and inhibits settling of reinforcement particles and in upper region sedimentation of reinforcement particles takes place and thus providing maximum concentration of binder particles in middle portion of ingot.

In powder metallurgy route, composites were synthesized at different concentrations of reinforcements (0%, 1%, 5%, 10%) by compaction and sintering, reinforcement boosted hardness at low concentration but low effects of sintering results in increased porosity and Al-HEA interface, thus decreasing hardness at higher concentration of reinforcement.

On comparing both the processes, Stir Casting provided better hardness results than Powder Metallurgy route.

Table of Contents

List of Figures

List of Tables

Chapter 1

Introduction

1. Metal Matrix Composites

A composite material can be defined as a combination of two or more materials that results in better properties than those of the individual components used alone. In contrast to metallic alloys, each material retains its separate chemical, physical, and mechanical properties. The two constituents are a reinforcement and a matrix. The main advantages of composite materials are their high strength and stiffness, combined with low density, when compared with bulk materials, allowing for a weight reduction in the finished part. The reinforcing phase provides the strength and stiffness. In most cases, the reinforcement is harder, stronger, and stiffer than the matrix. The reinforcement is usually a fiber or a particulate. Particulate composites have dimensions that are approximately equal in all directions. They may be spherical, platelets, or any other regular or irregular geometry. Particulate composites tend to be much weaker and less stiff than continuous fiber composites, but they are usually much less expensive. Particulate reinforced composites usually contain less reinforcement (up to 40 to 50 volume percent) due to processing difficulties and brittleness.

Composites are classified based on the types of matrix and reinforcements. Composites are classified as polymer matrix composites (PMCs), metal matrix composites (MMCs), and ceramics matrix composites (CMCs) based on the type of matrix. Depending on the types of reinforcements, composites include particle reinforced composites, short fiber composites (whisker), and continuous fiber composites (sheet). The materials for reinforcements can be organic fibers, metallic fibers, ceramic fibers, and particles. The materials for matrices can be polymers, metal and its alloys, glasses, glass-ceramics, ceramics. Usually, the strength of a matrix is considerably less than that of a fiber. Metal composite materials have found application in many areas of daily life for quite some time. Often it is not realized that the application makes use of composite materials. These materials are produced in situ from the conventional production and processing of metals. Here, the Dalmatian sword with its meander structure, which results from welding two types of steel by repeated forging, can be mentioned. Materials like cast iron with graphite or steel with a high carbide content, as well as tungsten carbides, consisting of carbides and metallic binders, also belong to this group of composite materials. For many researchers the term metal matrix composites is often equated with the term light metal matrix composites (MMCs).[1]

These innovative materials open up unlimited possibilities for modern material science and development; the characteristics of MMCs can be designed into the material, custom-made, dependent on the application. From this potential, metal matrix composites fulfill all the desired conceptions of the designer. This material group becomes interesting for use as constructional and functional materials, if the property profile of conventional materials either does not reach the increased standards of specific demands, or is the solution of the problem. However, the technology of MMCs is in competition with other modern material technologies, for example powder metallurgy. The advantages of the composite materials are only realized when there is a reasonable cost – performance relationship in the component production. The use of a composite material is obligatory if a special property profile can only be achieved by application of these materials.[1]

The possibility of combining various material systems (metal – ceramic – non metal) gives the opportunity for unlimited variation. The properties of these new materials are basically determined by the properties of their single components.

. The development objectives for light metal composite materials are:

• Increase in yield strength and tensile strength at room temperature and above while maintaining the minimum ductility or rather toughness,

• Increase in creep resistance at higher temperatures compared to that of conventional alloys,

• Increase in fatigue strength, especially at higher temperatures,

• Improvement of thermal shock resistance,

• Improvement of corrosion resistance,

• Increase in Young's modulus,

• Reduction of thermal elongation.[2]

2. High Entropy Alloys

Each high-entropy alloy contains multiple elements, often five or more in equiatomic or near-equiatomic ratios, and minor elements [3] The basic principle behind HEAs is that significantly high mixing entropies of solid solution phases enhance their stability as compared with intermetallic compounds, especially at high temperatures. This enhancement allows them

to be easily synthesized, processed, analyzed, manipulated, and utilized by us. In a broad sense, HEAs are preferentially defined as those alloys containing at least five principal elements, each having the atomic percentage between 5% and 35%. The atomic percentage of each minor element, if any, is hence less than 5% [3]

High entropy alloy system shows microstructural stability at room, cryogenic, and elevated temperatures, and shows better structural properties like higher tensile/compressive strength, fracture toughness, fatigue properties, and creep resistance and electrochemical properties (oxidation and corrosion resistance), as the consequence of the observed simple microstructure[4][5]. The introduction of the HEA concept accelerated the research in the field of materials science, where the concept of attaining simple solid solutions from multiple principal alloying elements have been established . Yeh et al. [5] illustrated that the addition of five or more principal alloying elements, each with an atomic percentage between 5 and 35 wt% could increase the configurational entropy at a random state (larger than 1.5R). Such an increase in configurational entropy reduces the Gibb's free energy of the alloy system and forms a simple solid solution with simple fundamental crystal structures (face-centered cubic (fcc), body-centered cubic (bcc) and hexagonal closest packed (hcp) or their combination) with reduced number of phases as expected by Gibb's phase rule. [1] From statistical thermodynamics, Boltzmann's equation [6] can be used for calculating configurational entropy of a system:

$$\Delta S_{conf} = k \ln w \quad \ldots (1)$$

where k is Boltzmann's constant and w is the number of ways in which the available energy can be mixed or shared among the particles of the system. Thus the configurational entropy change per mole for the formation of a solid solution from n elements with x_i mole fraction is:

$$\Delta S_{conf} = -R \sum_{i=1}^{n} X_i \ln X_i \quad \ldots (2)$$

Let us consider an equiatomic alloy at its liquid state or regular solid solution state. Its configurational entropy per mole can be calculated as follows :

$$\Delta S_{conf} = -k \ln w = -R \left(\frac{1}{n}\ln\frac{1}{n} + \frac{1}{n}\ln\frac{1}{n} + \ldots\ldots + \frac{1}{n}\ln\frac{1}{n}\right) = R \ln n \quad \ldots (3)$$

where R is the gas constant, 8.314 J/K mol.

From the above equation, ΔS_{conf} can be calculated as R ln 5 = 1.61R. For a non equiatomic HEA, the mixing entropy would be lower than that for an equiatomic alloy[5].

HEA particles are a good candidate as reinforcement for metal matrix composites. Some researches on HEA particles reinforced metal matrix composites have been reported. However, the preparation of aluminum matrix composites reinforced with HEA particles has been rarely reported[7].

2.1 FOUR CORE EFFECTS OF HEAs

There are many factors affecting microstructure and properties of HEAs. Among these, four core effects are most basic [3]. Because HEAs contain at least five major elements, and conventional alloys are based on one or two metal elements, different basic effects exist between these two categories. The four core effects are high entropy, severe lattice distortion, sluggish diffusion, and cocktail effects [6]

2.1.1 High Entropy Effects

It is the most important effect because it can enhance the formation of solid solutions and makes the microstructure much simpler than expected. HEA helps in the formation of solid solutions and makes the microstructure much simpler than expected. High entropy effect helps in the formation of simpler solid solutions in HEAs rather than formation of different intermetallics specially at higher temperatures [8].The high entropy effect facilitates the formation of disordered solid solution rather than ordered intermetallics compound. Elemental phases have small negative ΔH_{mix} and ΔS_{mix} because they are based on one major element. Compound phases have large negative ΔH_{mix} but small ΔS_{mix} because ordered structures have small configurational entropy. But random solid solution phases containing multicomponents have medium negative ΔH_{mix} and highest $\Delta S_{mix.}$

As the Gibbs free energy of mixing, $\Delta G_{mix,}$ is

$$\Delta G_{mix} = \Delta H_{mix} - T\Delta S_{mix}$$

Where ΔH_{mix} and ΔS_{mix} are the enthalpy of mixing and entropy of mixing, respectively, higher number of element would potentially lower the mixing free energy, especially at high temperatures by contributing larger $\Delta S_{mix.}$ Therefore, disordered solid solution phase is more stable at high temperature than ordered intermetallics phases. It enhances the formation of solid solution phase due to which solution hardening take place in solution phase causing increase in the strength and ductility of HEAs. The stronger bond energies will enhance the formation of solid solution rather than intermetallics.

2.1.2 Sluggish Diffusion effect

HEAs consist of random solid solution phases along with ordered solid solution, causing sluggish diffusion of atoms and vacancies leading to chemical stability of the HEAs. A vacancy in the whole solute matrix is in fact surrounded and competed by different element atoms during diffusion, It has been proposed that slower diffusion and higher activation energy would occur in HEAs due to larger fluctuation of lattice potential energy (LPE) between lattice sites. The abundant low-LPE sites can serve as traps and hinder the diffusion of atoms. This leads to the sluggish diffusion effect.

It is expected that sluggish effect might affect phase nucleation, growth and distribution, and morphology of new phase through diffusion controlled phase transformation.

This effect helps in improving the properties and microstructure of the HEAs. As sluggish diffusion leads to finer grain structure causing good toughness and strength. It also improves the creep property causing prolong life at high temperature.

2.1.3 Severe lattice distortion effect

It is important to note that due to multicomponent matrix of different solid solution phases in HEAs, each atom is surrounded by different kind of atom thus causing severe lattice strain and stress due to atomic size difference.

Along with different atomic size difference, different bonding energy and crystal structure of consisting elements also leads to higher lattice strain. Lattice distortion not only affects various properties but also reduces the thermal effect on properties. Lattice distortion causes significant electronic scattering leading to decrease in electrical conductivity of HEAs.

Lattice distortion caused by thermal vibration is less than the severe lattice distortion in HEAs causing it insensitive towards the change of temperature.

2.1.4 Cocktail effects

In HEAs, cocktail effect is used to emphasize the enhancement of the properties by at least five major elements. Because HEAs might have single phase, two phases, three phases, or more depending on the composition and processing, the whole properties are from the overall contribution of the constituent phases. This relates with the phase size, shape, distribution, phase boundaries, and properties of each phase. Moreover, each phase is a multicomponent solid solution and can be regarded as an atomic-scale composite. Its composite properties not only come from the basic properties of elements by the mixture rule but also from the mutual interactions among all the elements and from the severe lattice distortion. Mutual interaction and lattice distortion would bring excess quantities in addition to those predicted by the mixture rule. As a whole, “cocktail effect” ranges from atomic-scale multicomponent composite effect to microscale multiphase composite effect.

3. Applications of High Entropy Alloys

HEAs have such promising properties that they are considered as potential candidates for a wide range of applications such as high temperature, electronic, magnetic, anticorrosion, and wear-resistant applications. Many of these properties arise out of their unique structural feature, a multicomponent solid solution. In some cases, HEAs show nanoscale precipitates, which further enhance some of the properties of these alloys.

The improved corrosion behaviour could be attributed to the different chemical composition as well as the formation of a unique high entropy atomic structure with a maximum degree of disorder.[9]

HEAs have been explored for applications at high temperatures. Their performance as coating and structural materials at high temperatures depends on their creep behavior, stability of microstructure, and mechanical properties at elevated temperatures. Therefore, it is of critical importance to understand the thermal stability of phases and microstructure of HEAs.

BCC HEAs are important in high-strength applications as they usually show better mechanical properties like higher yield strength than FCC HEAs. Formation of BCC structure is favored when most of the binary pairs present in the alloy crystallize in BCC lattice[6]

In the current state, a number of advanced applications demanding new and improved materials include the following [3]

1. Engine materials: higher elevated-temperature strength, oxidation resistance, hot corrosion resistance, and creep resistance
2. Nuclear materials: improved elevated-temperature strength and toughness with low irradiation damage
3. Tool materials and hard-facing materials: improved room and elevated-temperature strength and toughness, wear resistance, impact strength, low friction, corrosion resistance, and oxidation resistance
4. Waste incinerators: improved elevated-temperature strength, wear resistance, corrosion resistance, and oxidation resistance
5. Chemical plants: improved corrosion resistance, wear resistance and cavitation resistance for chemical piping systems, pumps, and mixers
6. Marine structures: improved corrosion resistance and erosion in seawater
7. Heat-resistant frames for multifloor buildings: higher elevated temperature strength which could sustain during incidences of fire
8. Light transportation materials: improved specific strength and toughness, fatigue strength, creep resistance, and formability

In conclusion, HEAs and HE-related materials have potential applications in different fields and are expected to replace traditional materials in many sectors. In just a decade from 2004, extraordinary progress has been made.

4. Stir Casting

In stir casting we use stirrer to agitate the molten metal matrix. The stirrer is generally made up of a material which can withstand at a higher melting temperature than the matrix temperature. Generally graphite stirrer is used in stir casting. The stirrer is consisting of mainly two components cylindrical rod and impeller. The one end of rod is connected to impeller and other end is connected to shaft of the motor. The stirrer is generally held in vertical position and is rotated by a motor at various speeds. The resultant molten metal is then poured in die for casting. Stir casting is suitable for manufacturing composites with up to 30% volume fractions of reinforcement.[10]. A major concern in associated with the stir casting is segregation of reinforcement particles due to various process parameters and material properties result in the non-homogeneous metal distribution. The various process parameters are like wetting condition of metal particles, relative density, settling velocity etc. The distribution of particle in the molten metal matrix is also affected by the velocity of stirrer, angle of stirrer, vortices cone etc. In this method first the matrix metal is heated above its liquid temperature so that it is completely in molten state. After it is cooled down to temperature between liquid and solidus state means it is in a semi-solid state. Then preheated reinforcement particles are added to molten matrix and again heated to fully liquid state so that they mixed thoroughly each other

4.1 Factors Affecting Process

Information collected through various research papers show the following factors which affect the stir casting process the most. They are

1. Speed of stirring

2. Time duration of stirring

3. Stirring temperature [10]

5. Powder Metallurgy

Powder metallurgy (PM) is the production and utilization of metal powders. Powders are defined as particles that are usually less than 1000 nm (1 mm) in size**.** Powders have a high ratio of surface area to volume and this is taken advantage of in the use of metal powders as catalysts or in various chemical and metallurgical reactions. The three main reasons for using PM are economic, uniqueness, and captive applications, Powder metallurgy parts are used in engine, transmission, and chassis applications. Sometimes it is a unique microstructure or property that leads to the use of PM processing: for example, porous filters, self-lubricating bearings, dispersion strengthened alloys, functionally graded materials, and cutting tools from tungsten carbide or diamond composites. Powder metallurgy processing offers many advantages.

The PM process is material and energy efficient compared with other metal forming technologies. Powder metallurgy is cost effective for making complex-shaped parts and minimizes the need for machining. A wide range of engineered materials is available, and through appropriate material and process selection the required microstructure may be developed in the material. Powder metallurgy parts have good surface finish and they may be heat treated to increase strength or wear resistance. The PM process provides part-to-part reproducibility and is suited to moderate-to-high volume production.[11]

For the production of PM parts in high volumes, compaction is carried out in rigid dies. In most instances, the metallic powders are mixed with a lubricant to reduce inter particle friction during compaction and to facilitate ejection of the compacted parts by reducing friction at the die-wall and core-rod interfaces. The metal powders may be elemental powders; mixtures of elemental powders; or mixtures of elemental powders with master alloys or ferroalloys, pre alloys, diffusion alloys, or hybrid alloys. A consequence of the various alloying methods available is that only the PM materials made from pre alloyed powders are chemically homogeneous. The other alloying methods can result in chemically inhomogeneous materials. The hardenability is determined by the local chemical composition, and the resulting microstructures are generally quite complex. Chemical analysis can be a challenge due to the inhomogeneous nature of the materials. While the objective is generally to achieve a density as uniform as possible throughout the compacted part. The position of the neutral zone may be adjusted by varying the pressure exerted by the upper and lower punches. Compaction in rigid dies is limited to part shapes that can be ejected from the die cavity. Parts with undercuts, reverse tapers, threads, and so forth, are not generally practical. Such features are formed by post sintering machining operations. Some PM parts are molded (shaped) rather than

compacted. The process makes complex shaped, small-to-medium sized PM parts with high relative densities. Some metal powders are not very compressible. The powder particles are hard and have limited plasticity. Rigid die compaction is not suitable for consolidating such powders, and they must be processed by other means such as hot pressing, extrusion, or hot isostatic pressing (HIP) Highly reactive metal powders are also not suitable for rigid die compaction. They generally need to be vacuum hot pressed, or encapsulated and extruded, or HIPed. Rigid die compacted parts and MIM parts are thermally treated to increase their strength in a process known as sintering. The parts are heated, generally in a reducing atmosphere, to a temperature that is below the melting point of the primary constituent of the material, in order to form metallurgical bonds between the compacted metal powder particles. Sintering is a "shrinkage" process. The system tries to reduce its overall surface area via various diffusion processes. Metallurgical bonds (microscopic weldments) form between adjacent metal particles (after oxides have been reduced on the surface of the powder particles), pore surfaces become less irregularly shaped, and larger pores grow at the expense of the smaller pores.[11]

6. Thesis Objective

The main objectives of this research work are as follows

1. Preparation of FeCrAlMnNi High Entropy Alloy powder by ball milling
2. Characterization of HEA powder
3. Synthesis of Al-HEA composite by stir casting at different compositions
4. Investigation of microstructures and hardness of prepared composite samples
5. Investigation of cooling effect and sedimentation during solidification of melt
6. Synthesis of Al-HEA composites by Powder metallurgy at different composition
7. Investigation of microstructures and hardness of prepared composite samples
8. Comparison of Properties observed by different routes

7. Thesis Outline

The research work has been divided systematically into 6 chapters to give detailed information of the research conducted, from the introduction of metal matrix composites and high entropy alloys to results and discussions observed by mixing them.

The chapter content are as follows:

1. **Chapter 1, Introduction** : Overview of metal matrix composites and introducing FeCrAlMnNi HEA as a reinforcement, having wide range of applications and richness in properties by liquid and solid processing routes

2. **Chapter 2, Literature Survey**: deals with different fabrication techniques used for preparing Al composites with different reinforcement materials and their observed properties.

3. **Chapter 3, Characterization Techniques**: contains details about different characterization tools used for the study of composites and presents their working setup and working principle behind the tool to analyse the material.

4. **Chapter 4, Experimental Methods and Analysis**: emphasize the steps involved in the preparation of High Entropy Alloy powder and the composites formed by reinforcing it in Al Matrix.

5. **Chapter 5, Results and Discussions**: deals with the study of HEA reinforced Al based composites with the help of various characterization techniques.

6. **Chapter 6, Summary, Conclusion and Future scope:** summing up all the results of this thesis an overall conclusion is derived while outlining the future work to be done for further study.

Chapter 2

Literature Survey

Reinforcement plays a crucial role in determining the properties of the composite. Researchers have investigated the effects of reinforcing different types of reinforcement such as ceramic materials (Al_2O_3, SiC, B_4N, Carbon Nanotubes etc.)[12][4][13] including hybrid materials such as SiC+Graphene, Carbon Nanotubes + Fly Ash,[14] through different processing routes like solid state processing methods like mechanical mixing for different time intervals, spark plasma sintering and liquid state processes like stir casting, squeeze casting etc. and have observed an appreciable increase in mechanical properties of different Al grades.

As discussed in the above chapter High Entropy Alloys are rich in mechanical and thermal properties and have wide range of advanced applications.

Some processes like squeeze casting and spark plasma sintering can be complicated and are not economically favourable, thus, the process for fabrication was chosen be simple and economical.

Among the variety of manufacturing processes available for discontinuous metal matrix composites, stir casting is generally accepted as a particularly promising route, currently practiced commercially. Its advantages lie in its simplicity, flexibility and applicability to large quantity production with cost advantage.

Powder metallurgy is one of the most widely used fabrication techniques. Powder Metallurgy (P/M) offers designers and users a versatile and efficient method of producing components. The process is versatile because it can be used for simple and complex shapes, and a full range of chemical, physical and mechanical properties is possible to obtain. P/M is efficient because it produces moderate to high-volume net or near-net shapes, with very little raw material loss. In general, the process has very good potential to improve performance through uniform properties, fine grain structures, and chemical homogeneity.

Hence, the above two processes were used for the fabrication of Al based composite samples.

- **Choosing FeCrAlMnNi High Entropy Alloy as Reinforcement**

High entropy alloys (HEAs), a new type of materials, are composed of five or more principal elements with the concentrations ranging from 5 to 35 [6]. HEAs possess high strength, good structural stability and exceptional high-temperature strength. Recently, Jian Chen in [15] Compression tests show that the AlCoNiCrFe high-entropy alloy has a better strengthening effect than metallic glasses. However, only a few literatures have been reported on the MMCs reinforced by HEAs alloy so far.

Hardness of FeCrAlMnNi was found to be (4.0 Gpa) [16]FeCrAlMnNi HEA alloy was chosen in this investigation.

The FeCrAlMnNi HEA was prepared by mechanical alloying and the FeCrAlMnNi HEA particle-reinforced Al matrix composites were fabricated by powder metallurgy method and stir casting techniques.

Matrix + Reinforcement/s	Hardeness Measured	Tensile Strength	Processing Route	Reference
Al-6063 alloy Al-6063+5%TiB2 Al-6063+10%TiB2	80Hv 95Hv 110Hv		In-Situ Technique	[17]
Al-6061 alloy Al-6063+12%TiB2	62.8BHN 88.6BHN	134.8MPa 173.6MPa	In-Situ Technique	[18]
A390 alloy A390+3wt%TiB2	(300°C Temp) 68.0HRB 78.6HRB	(300°C Temp) 89.MPa 102.1MPa	In-Situ Technique	[19]
AA-7075 alloy AA-7075+3%TiB2 AA-7075+6%TiB2 AA-7075+9%TiB2	65VHN 80VHN 105VHN 125VHN	145MPa 195MPa 240MPa 280MPa	In-Situ Technique	[20]
Al-6061 alloy Al-6063+3%TiB2 Al-6063+6%TiB2 Al-6063+9%TiB2 Al-6063+12%TiB2	40.4VHN 57.5VHN 65.5VHN 76.8VHN 89.6VHN	178MPa 198MPa 207MPa 219MPa 210MPa	Two Step Stir Technique	[21]
Al-6061 alloy Al-6061+10%SiC+0%TiB2 Al-6061+10%SiC+2.5%TiB2 Al-6061+10%SiC+5%TiB2	45VHN 71VHN 75VHN 72VHN	150MPa 54MPa 97MPa	Stir Casting	[22]
Al-6061 alloy Al-6061+10%TiB2 Al-6061+20%TiB2 Al-6061+10%TiB2+2%gGr Al-6061+20%TiB2+2%Gr	62.93VHN 75.56VHN 84.46VHN 77.02VHN 91.42VHN	125MPa 150MPa 175MPa 179MPa 160MPa	Stir Casting	[21]

A356 alloy A356+0.5 vol.% nanoTiB2 A356+1.5 vol.% nanoTiB2 A356+3 vol.% nanoTiB2 A356+5 vol.% nanoTiB2 A356+0.5 vol.% microTiB2 A356+1.5 vol.% microTiB2 A356+3 vol.% microTiB2 A356+5 vol.% microTiB2		237MPa 241MPa 277MPa 258MPa 241MPa 223MPa 237MPa 271MPa 244MPa	Stir Casting	[23]
Al TiB2/Al Mg2Si/Al TiB2+Mg2Si/Al		66MPa 147MPa 201MPa 217MPa	In-Situ Technique	[24]
Al6061 Al 6061 + HEA(10h) Al 6061 + HEA(20h) Al 6061 + HEA(40h)	85BHN 92BHN 87BHN 97BHN	225Mpa 300Mpa 275Mpa 350Mpa	Ball Milling	[7]
PM6061 PM6061 (MM) PM 6061 + 5% AlN (MA) PM 6061 + 15% AlN (MA) PM 6061 + 5% Si3N4 (MA)	65HV 174HV 192HV 196HV 209HV		Ball Milling	[25]
Al6061 + SiC 5% Al6061 + Al2O3 3% Al6061 + TiB2 2%	122.7HV 138.1HV 105.6HV		Stir Casting	[22]
Al- 6061+ 3%Sic + 2%TiB2 Al- 6061+ 5%Sic + 5%TiB2	48HRB 68HRB	158.28 Mpa 155.90 Mpa	Stir Casting	[26]

Table 1. Literature Review Al based composites by different synthesis methods with synthesis parameter involved in it.

Chapter 3

Characterization Techniques and Methodology

1. X – Ray Diffraction (XRD)

X-Ray Diffraction (XRD) is a characterization tool to study the crystallographic structure, lattice parameters, strain, orientation of crystals, phase, etc. of material by use of X-rays, as the interatomic distance i.e. d-spacing of all matter is of the same order as of X-ray Wavelength. This technique is simple, reliable and non-destructive.

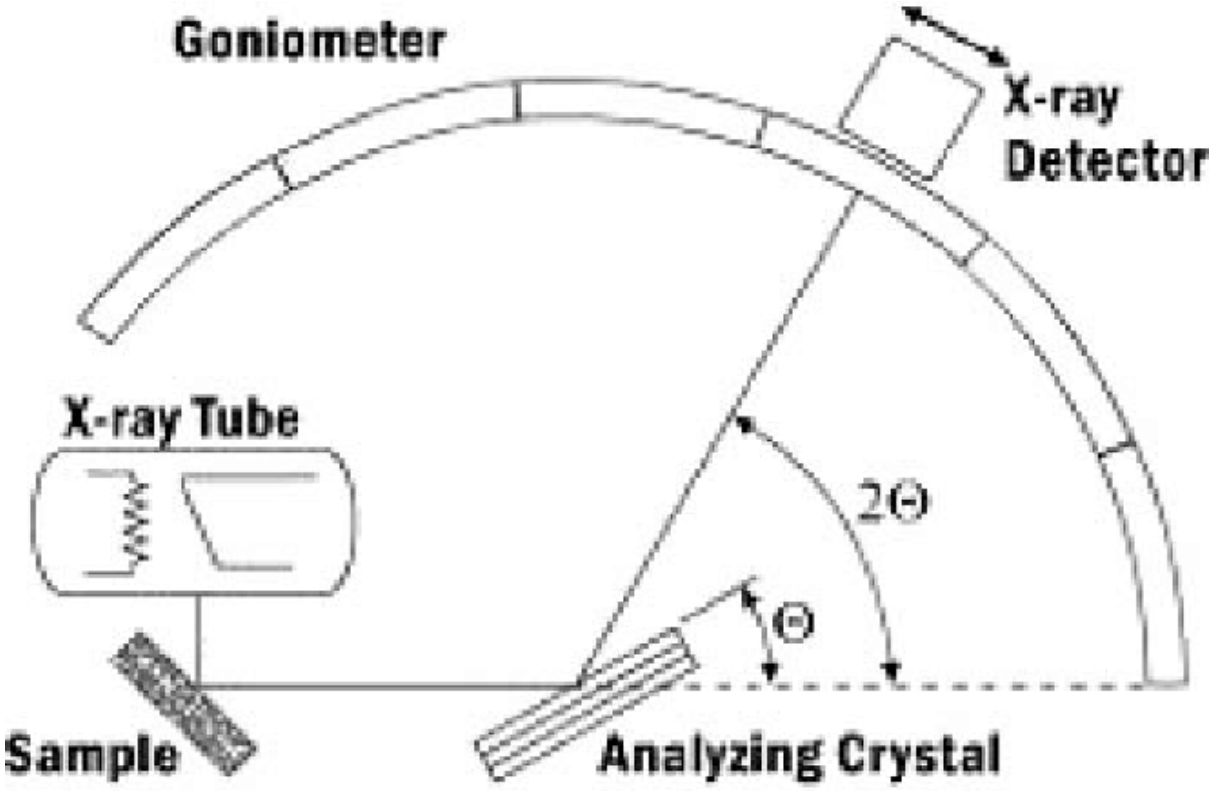

Fig 1. – Representation of typical X ray Diffraction [27]

In this technique, a collimated X-ray beams incidences on the sample material, atoms inside the material diffracts the X-rays beams depending on the d-spacing, according to Braggs law.

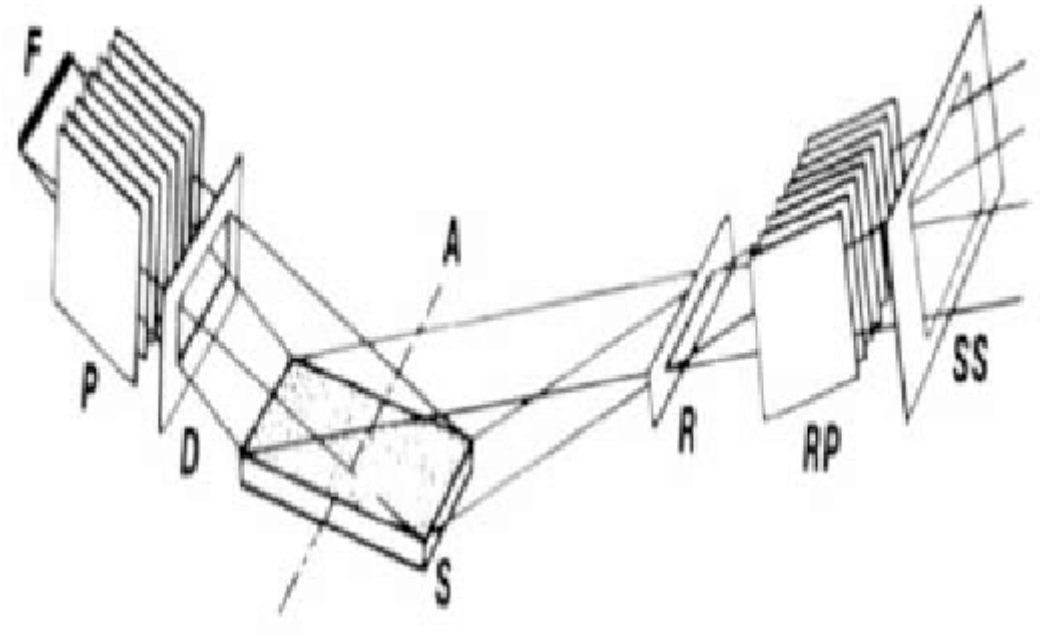

Fig. 2- Geometry of the Bragg-Brentano diffractometer.[27]

According to Braggs law,

$$N\lambda = 2d\sin\Theta \quad \text{…….(1)}$$

Where n being an integer, λ is X-ray beam wavelength, d is the interplanar distance of the crystal, Θ is the angle made by the atomic plane of the crystal and incidental X-ray beam. An XRD pattern can be plotted between the intensity of resultant of the diffracted peak on the y-axis and angular position of those peaks on the x-axis. Different materials have a different plane orientation with different d-spacing, depicting different XRD patterns, this XRD pattern can be said as a unique signature for a material. By comparing this XRD pattern, with the standard XRD files published by International Centre for Diffraction Data (ICDD), the structure and material composition can be determined, further studying of the XRD pattern lattice parameter, strain, particle size can be determined, etc.

In this research work, XRD measurements are done using Bruker D8 Advance X-Ray Diffractometer, with Cu Kα filtered radiation source having wavelength 1.5406 Å, recording the diffraction pattern between 20^{o}-90^{0} range of 2Θ.

2. Field Emission Scanning Electron Microscopy (FESEM)

FESEM is a characterization tool for morphological analysis of the material, being a non-destructive and non-contact technique for imaging the nanostructures. In this Microscopy technique, a tungsten filament cathode coupled with an electron gun is used to thermionically emit the Electron beam. Tungsten is generally used due to its low Vapour pressure and high

melting point among other metals. This electron beam passes through the anode which is positively charged, placed such that it accelerates the Electron beam and focuses it on the material in a raster pattern with the help of condenser lens placed just above the material, the Electron beam then collides with the material and emits back the signal which is detected by the detector. Figure 3.3 shows the schematic arrangement of the FESEM.

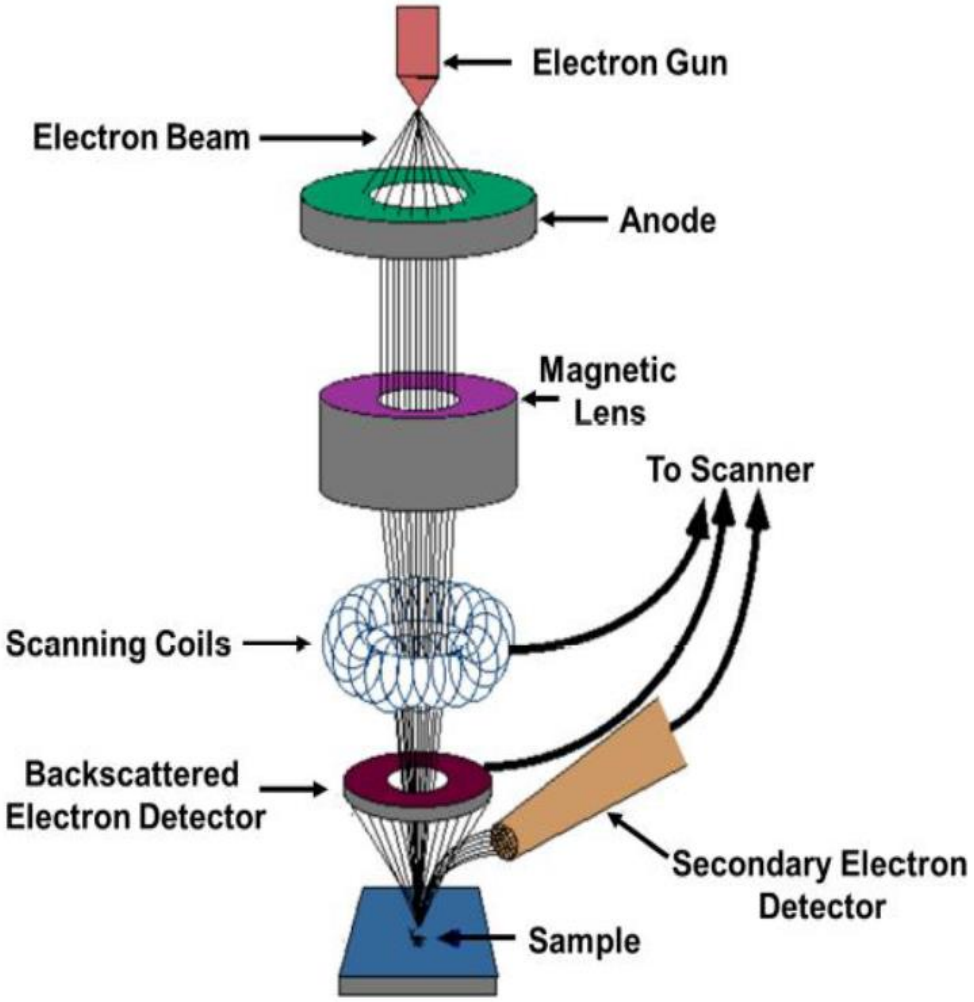

Fig. 3 - Schematic arrangement of FESEM [28]

When an electron interacts with the material it emits Secondary electrons (SE), Backscattered Electron (BSE), Auger Electrons, X-rays, etc.as shown in figure 3.4. But in FESEM, signals of Secondary Electron (SE) and Backscattered Electron (BSE) are detected by the detector to generate the images of nanostructure of material.

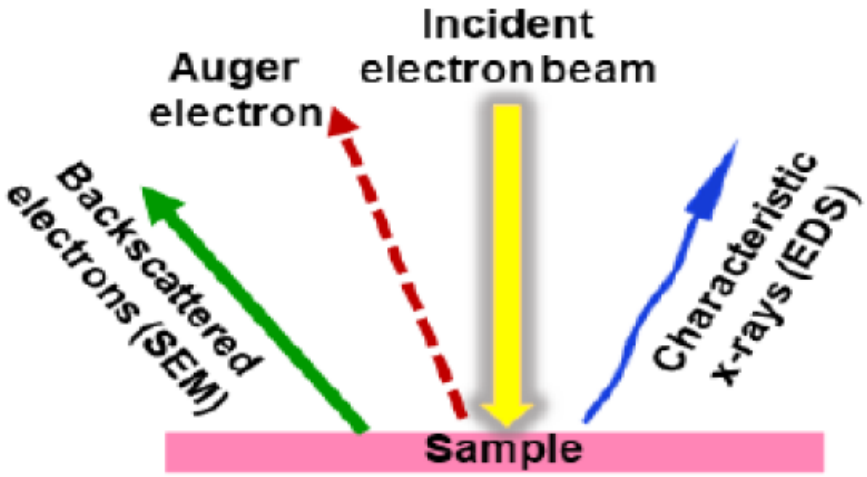

Figure 4. Interaction of electron with the material.[29]

a) Secondary Electron:
They are generated due to the inelastic collision of an incident electron with the atom of the surface material, depth of which can be less than 100nm to 5μm, this electron has low energy less than 50eV.

b) Backscattered Electron:
They are generated due to the elastic collision of the incident electron with the atom of the material in the bulk, depth of the penetration of incident electron beam depends on its energy, atomic density, and atomic number, this electron beam changes its path after the interaction, it has high energy more than 50 eV.
In this research work, FESEM is done by JEOL JSM-7610F PLUS.

3. Energy Dispersive Spectroscopy (EDS)

The energy dispersive spectroscopy (EDS) technique is mostly used for qualitative analysis of materials but is capable of providing semi-quantitative results as well. Typically, SEM instrumentation is equipped with an EDS system to allow for the chemical analysis of features

being observed in SEM monitor. Simultaneous SEM and EDS analysis is advantageous in failure analysis cases where spot analysis becomes extremely crucial in arriving at a valid conclusion. Signals produced in an SEM/EDS system includes secondary and backscattered electrons that are used in image forming for morphological analysis as well as X-rays that are used for identification and quantification of chemicals present at detectable concentrations.

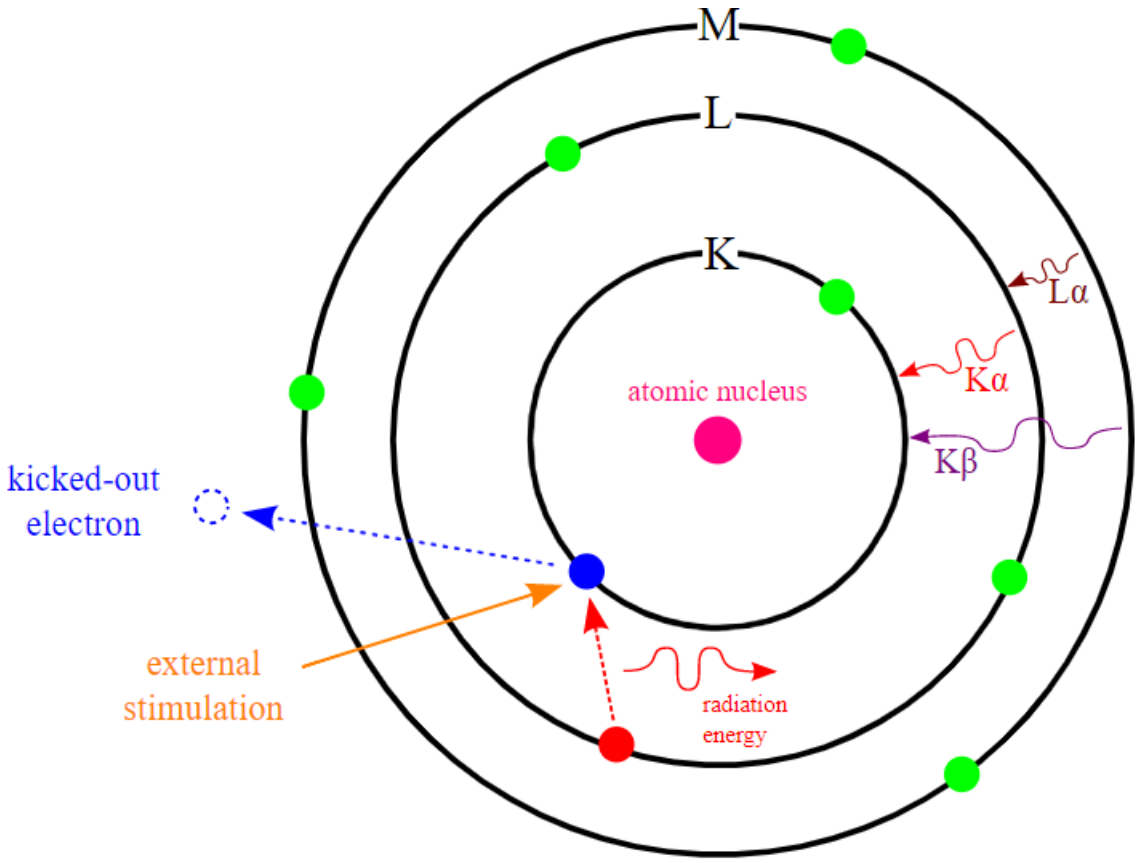

Fig. 5 – Principal of EDS

The detection limit in EDS depends on sample surface conditions, smoother the surface the lower the detection limit. EDS can detect major and minor elements with concentrations higher than 10 wt% (major) and minor concentrations (concentrations between 1 and 10 wt%). The detection limit for bulk materials is 0.1 wt% therefore EDS cannot detect trace elements (concentrations below 0.01 wt%). EDS technique is capable of producing elemental distribution maps.

4. Brinell Hardness Test

As defined in ASTM E10-18, a Brinell hardness test is “an indentation hardness test using a verified machine to force an indenter (tungsten carbide ball with diameter D), under specified conditions, into the surface of the material under test.” Following this initial step, the diameter of the resulting indentation d from the force is measured in at least two directions perpendicular to each other. The mean of these measurements is the Brinell hardness value.

This differs from alternative indentation hardness testing methods such as the Vickers, Rockwell, and Knoop tests, as well as those practiced for assessing scratch and rebound hardness types.

The Brinell method applies a predetermined test load (F) to a carbide ball of fixed diameter (D) which is held for a predetermined time period and then removed. The resulting impression is measured with a specially designed Brinell microscope or optical system across at least two diameters – usually at right angles to each other and these results are averaged (d). Although the calculation below can be used to generate the Brinell number, most often a chart is then used to convert the averaged diameter measurement to a Brinell hardness number. Typically the greatest source of error in Brinell testing is the measurement of the indentation. Due to disparities in operators making the measurements, the results will vary even under perfect conditions. Less than perfect conditions can cause the variation to increase greatly. Frequently the test surface is prepared with a grinder to remove surface conditions

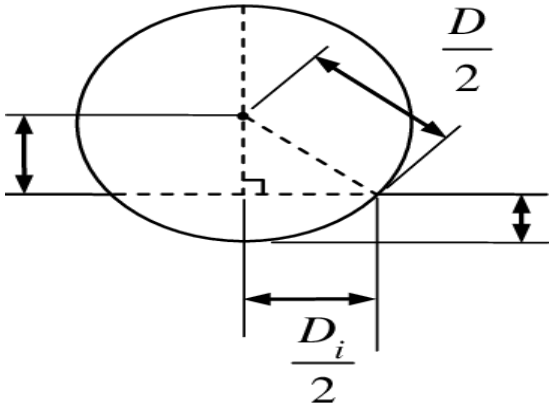

Fig. 6 – Schematic of Brinell Hardness Test [30]

$$HB = \frac{2F}{\pi D(D - \sqrt{D} - d)}$$

Where,

D = Ball diameter

d = Impression diameter

F = Load

HB = Brinell result

We conducted the brinell test by Samarth engineering brinell tester.

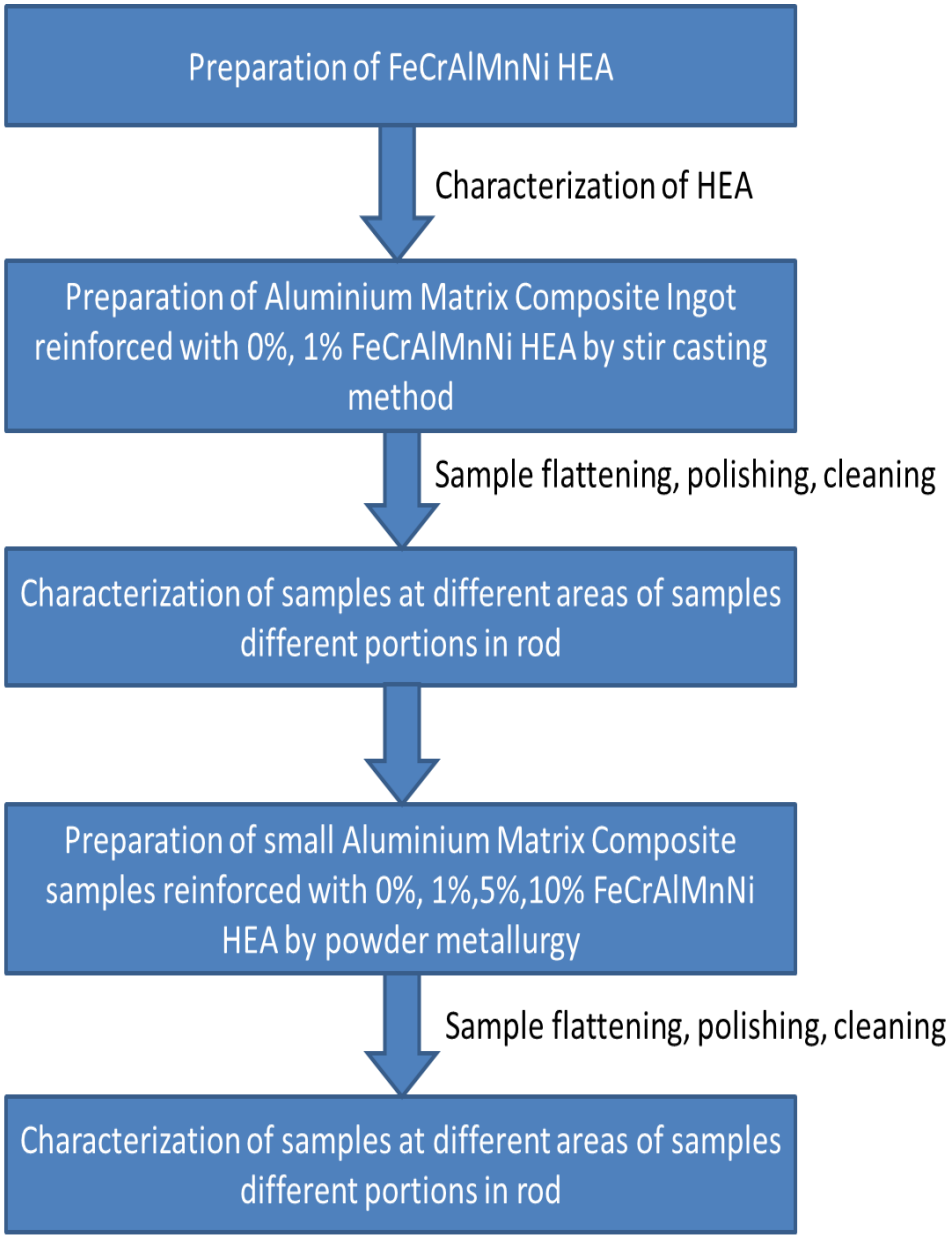

Fig.7 - Methodology involved in experiment

3.1 Preparation of FeCrAlMnNi High Entropy Alloy

Powder sample is prepared using high-energy ball milling from pure materials (with 98%–99.9% purity). The metallic elements (total 40 g) are kept in milling vial (capacity of 250 cm^3) with 41 tungsten coated balls maintaining 10:1 BPR (Ball to Powder Ratio) along with the process control agent (PCA), i.e. toluene C_7H_8 for preventing cold welding during milling process. A Fritsch pulverisette 6 planetary ball mill was used to pulverize the sample with the speed of 300 rpm for 20 h (with clockwise 30 min milling time afterward 15 min dwells and again 30 min with anti-clock rotation). And thermodynamical parameters were calculated.

The enthalpy of HEA is calculated as $\Delta H_{mix} = \sum_{i=1}^{n} \Omega i, jCi\ Cj$

Where n is the number of mixing element, $\Omega i,j = 4\Delta H_{mix}^{AB}$ is a regular solution interaction parameter between the i^{th} and j^{th} elements and C_i or C_j is the atomic % of the components. ΔH_{mix}^{AB} (kJ/mol) is the enthalpy of the mixing calculated by Miedema's model for binary atomic pairs.

The entropy of the mixing $(\Delta S)_{mix}$ can be calculated as (2) $\Delta S_{mix} = -R \sum_{i=1, i\neq j}^{n} Ci \ln Ci$ Where C_i is the atomic percentage (%) of the ith component $\sum_{i=1}^{n} C_i = 1$ and R = 8.314 J/KMol is the gas constant.

For the prediction of solid-solution formation for various type of high entropy alloys, a parameter Ω was defined as $\Omega = \frac{Tm\Delta Smix}{|\Delta Hmix|}$

Where T_m is the melting temperature of n element, was considered by the rule of mixtures $T_m = \sum_{i=1}^{n} C_i(T_m)_i$, Where $(T_m)_i$ is the melting point of the i^{th} component of alloy.

Another parameter, which denote the compressive effect due to the atomic size mismatch difference in the n-element alloy can be calculated as

$$\delta = 100\sqrt{\sum_{i=1}^{n} c_{i=1} c_i \left(1 - \frac{r_i}{\bar{r}}\right)^2}$$

Here, C_i is the atomic percentage of the i^{th} component and $\bar{r} = \sum_{i=1}^{n} C_i r_i$ is the average atomic radius and r_i, the atomic radius [29].

It is observed that, FCC phase is more stable at higher VEC (≥8) and BCC phases are more stable at lower VEC (≤6.87). In the range between both conditions ($6.87 \geq VEC \leq 8$), mixed BCC and FCC will present [31]. It can be defined with the help of the following relation: $VEC = \sum_{i=1}^{n} C_i(VEC)_i$

While $(VEC)_i$ is the Valency electron concentration of the individual element. All the thermodynamic parameters for FeCrAlMnNi HEA are given in Table 2.

Alloy	ΔH_{mix} (KJ/mol)	ΔS_{mix} ($JK^{-1}mol^{-1}$)	T_m(°C)	Ω	r(Å)	VEC
FeCrAlMnN	2.645	1.792R	1698	11.1	5.391	5.312

Table 2 – Estimated thermodynamical and physiochemical properties of FeCrAlMnNi HEA

3.2 Preparation of Aluminium Matrix Composite reinforced with 1% FeCrAlMnNi HEA :-

The material matrix used for present study is pure Aluminium (99.99%) .The FeCrAlMnNi HEA with above mentioned physiochemical and thermodynamical properties are being used as

reinforcement for the preparation of composite. Stir casting was done using SwampEquip Bottom Pouring stir casting machine.1100 gm of pure Aluminium wires was charged into a hot crucible and superheated to 800°C in an electrical resistance furnace. The furnace temperature was controlled by digital temperature controller system. HEA reinforcement (11.11 gm) were preheated to 200°C to remove moisture and adsorbed gases from the particles surface. Preheated HEA particles were introduced to the vortex of molten metal. After the introduction of reinforcement, mechanical stirring was carried at out for 15 minutes at the speed of 300 rpm. Composite mixture was poured into permanent die steel moulds, which was preheated to 200°C to remove any moisture, having 30 mm diameter and 300 mm length.

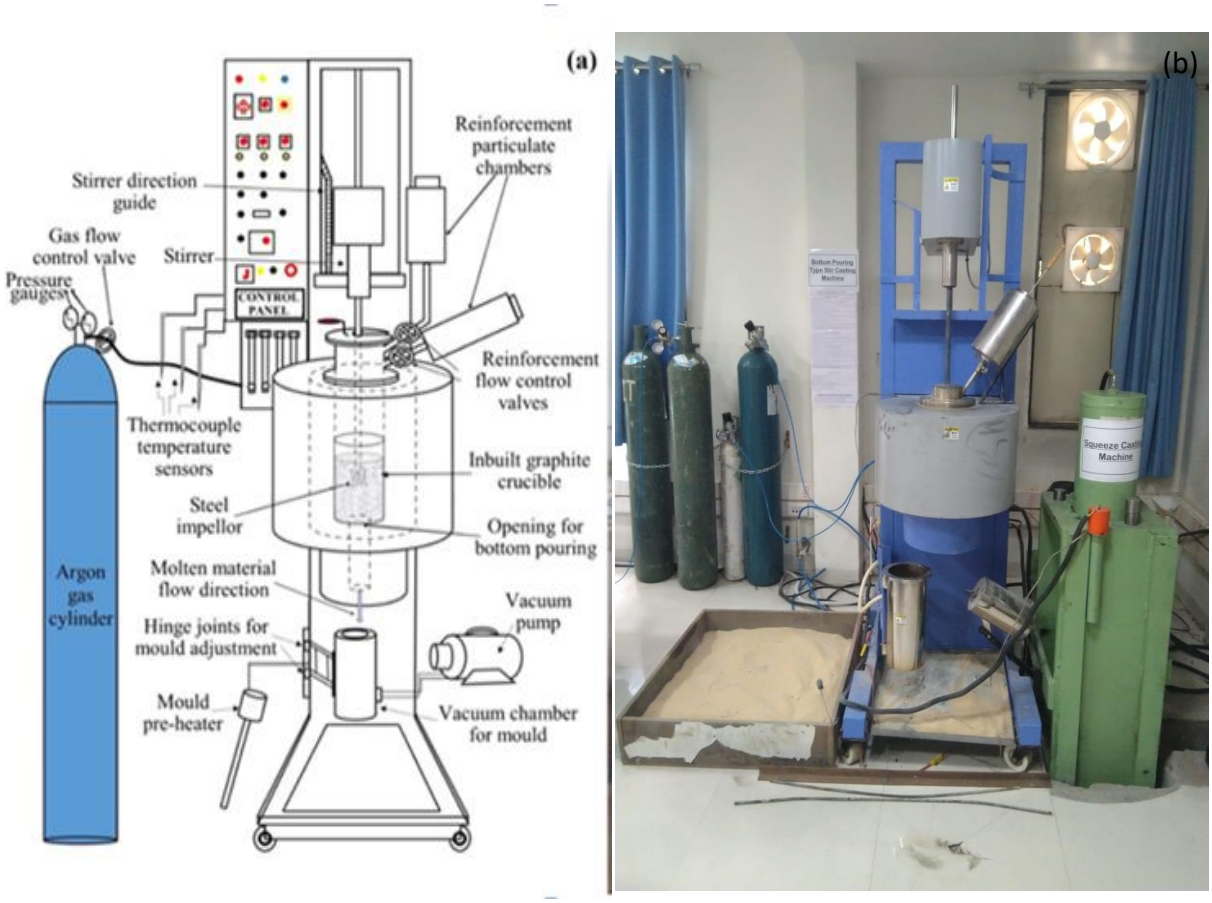

Fig. 8 (a) Schematic diagram of gas injection bottom pouring vacuum stir casting[32] and (b) actual images of casting unit used for casting

3.3 Characterization of HEA powder and composite samples

Specimens of 30mm diameter and 12 mm length were cut from 3 portions (Top, Middle, Bottom) of the cast ingot. For XRD (Bruker D2 PHASER, CuKα) analysis, a plot of 2-theta verses intensity was analyzed using origin plus software. To investigate the mechanical behaviour of the composites the hardness tests were carried out using Brinell hardness tester(Samarth Engineering) at 3 areas on each sample to investigate the non uniformity in

distribution of HEA particles which can occur due to cooling effect, sedimentation etc.. Indentations on specimen were made by 5mm carbide steel ball under minor force of 750 KgF and results were calculated on B scale. Microstructural studies conducted using Optical microscopy(ZEISS Axio Vert.A1). A Scanning Electron Microscope (SEM, FESEM, Carl Zeiss supra 55) is used to study surface morphology of HEA and composite.

3.4 Synthesis of composite samples by Powder Metallurgy

Synthesis was done in following steps:-

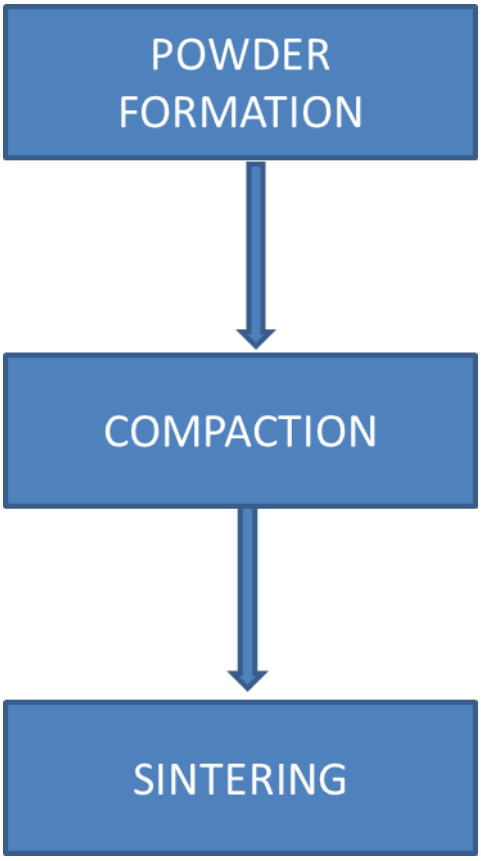

Fig. 9 – Flow Chart of Synthesis of Composite by Powder Metallurgy

3.4.1 Powder Formation

Gas Atomized Al powder was mixed with 20hr milled FeCrAlMnNi High Entropy Alloy. The metallic elements (total 40 g) are kept in milling vial (capacity of 250 cm^3) with 41 tungsten coated balls maintaining 10:1 BPR (Ball to Powder Ratio) along with the process control agent (PCA), i.e. toluene C_7H_8 for preventing cold welding during milling process. A Fritsch pulverisette 6 planetary ball mill was used to pulverize the sample with the speed of 300 rpm for 1h (with clockwise 30 min milling time afterward 15 min dwells and again 30 min with anti-clock rotation), to avoid mechanical alloying between Al matrix and HEA reinforcement.

3.4.2 Compaction And Sintering

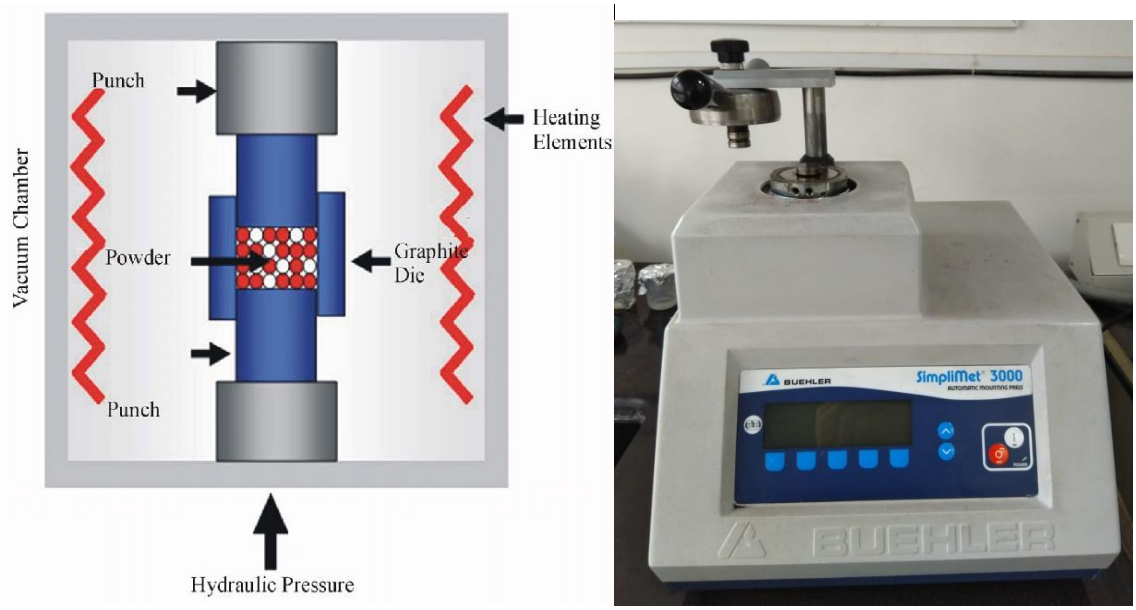

(a) (b)

Fig.10– (a) Schematic figure of Hot Press and (b) Instrument used for compaction

For 10gm powder of each composition, compaction was done using BUEHLER SIMPLIMET 3000 pressing machine at temperature of 160^{O}C under pressure of 180Mpa.

Compaction formed cylindrical green body of composites with 10gm each weighing 10gm.

Sintering of all 4 samples was done together under vacuum conditions at 600^{O}C temperature in NABERTHERM SPLIT TUBE FURNACE MODEL “RSV 120/500/13.

Chapter 4

Results and Discussions

4.1 Analysis of FeCrAlMnNi Powder

XRD patterns of alloy sample are obtained by powder diffractometer using CuKα radiation source at a different time interval of ball milling process. Fig. 4.1 shows the XRD patterns of FeCrAlMnNi HEA powders under the various ball milling duration of each 5 h intervals. Peaks reveal that the HEA powder formed has BCC phase. It can be seen that the intensities of peaks are lowered after 20 h milling, it may be due to the desolation of lower melting point elements with highest melting point elements. Apart from that, there is no other shifting of the peak observed. The broadening of the peak is due to lattice distortion, which may be due to the induced strain of excessive grain refinement by the frequent cold deformation of the powder [31]. Crystallite size(τ) was calculated using Scherrer equation [33] and tabulated in table 1.

Time	10mins	5Hrs	10Hrs	15Hrs	20Hrs
τ(nm)	20.49	9.93	5.04	5.029	5.279

Table 3 : crystallite sizes after different time intervals of milling

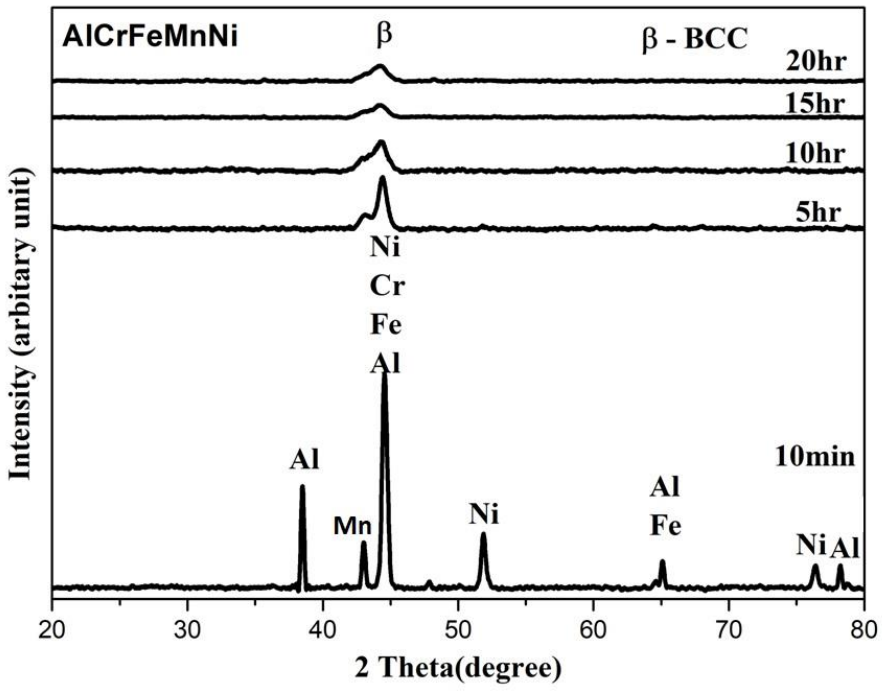

Fig. 11 – XRD of AlCrFeMnNi at different time intervals

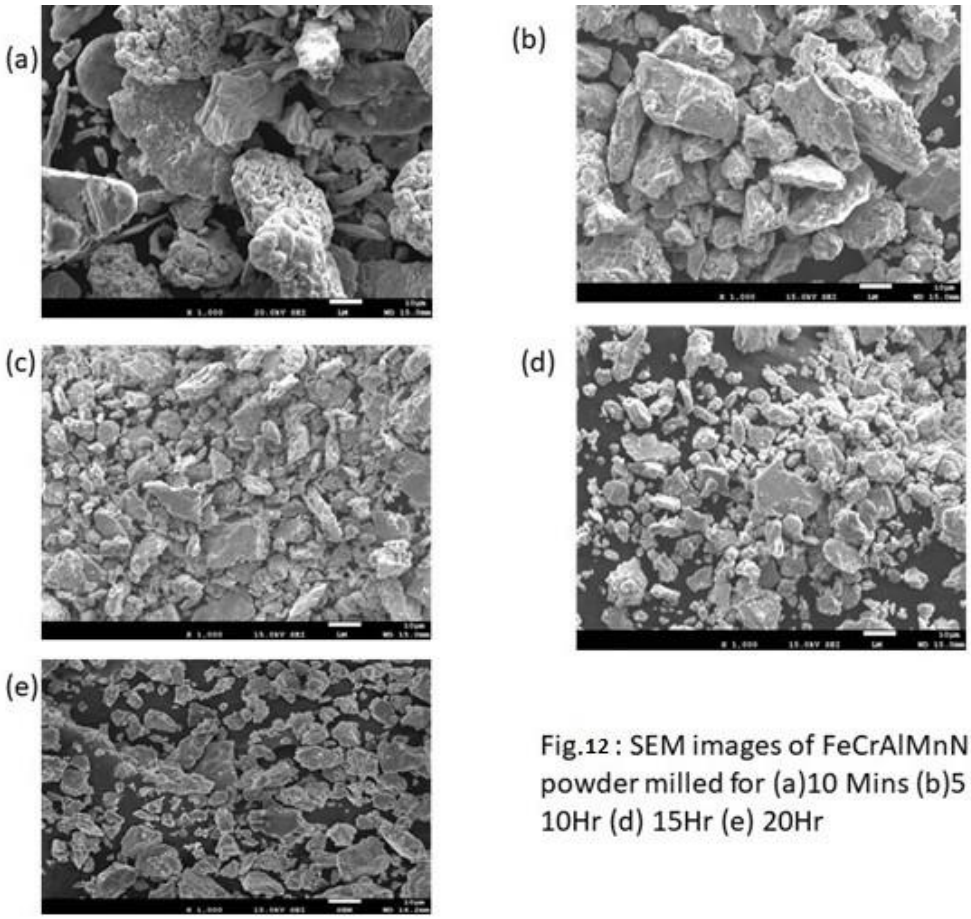

Fig.12 : SEM images of FeCrAlMnNi HEA powder milled for (a)10 Mins (b)5 Hr (c) 10Hr (d) 15Hr (e) 20Hr

4.2 Analysis of Composite prepared by stir casting

XRD patterns for pure aluminium and the HEA reinforced aluminium matrix composite are shown in fig. 2. No peaks of FeCrAlMnNi appear in the scan of the 1% wt. composite sample which indicates either no or a limited interfacial reaction that possibly was not detected due to limited resolution of XRD instrument at this small content[12].

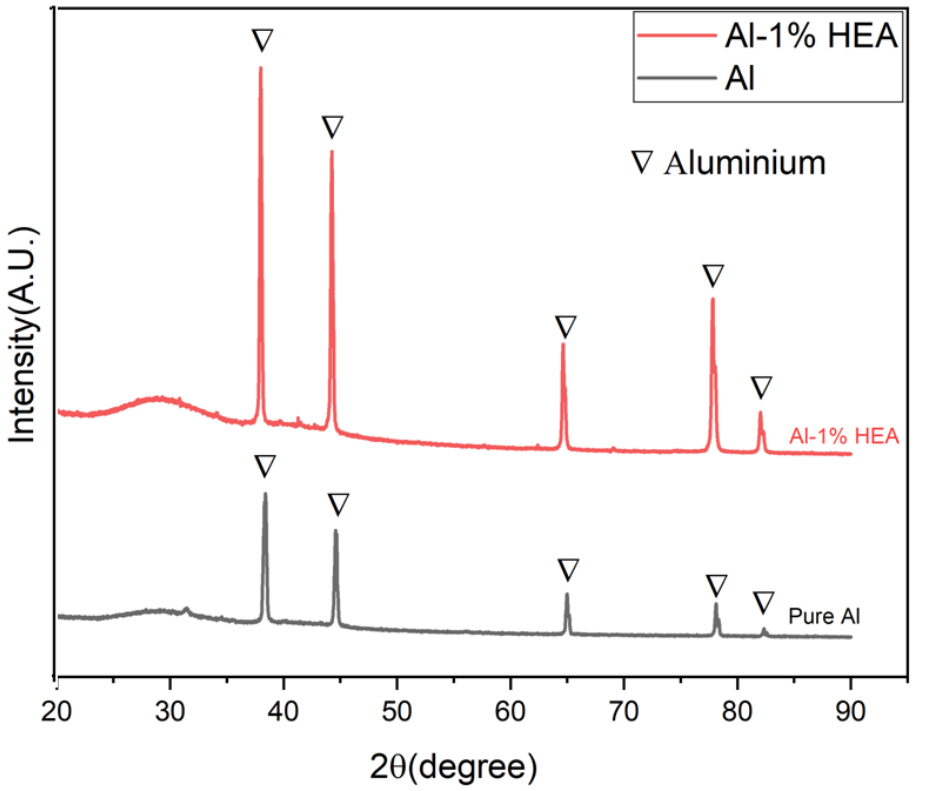

Fig. 13 – XRD scans of Pure Aluminium and Al – 1wt% HEA

4.2.1 Microstructure analysis of composite

Microstructures of small specimen of Al and Al-1%HEA are shown in fig. 4 and fig. 5. Microstructure clearly reveals that most the reinforcement high entropy particles are collected at grain boundaries of aluminium, which is responsible for hardening of Al. The microstructure is composed of an aluminium matrix containing BCC phased FeCrAlMnNi High entropy particles. In general the HEA powder is not uniformly distributed, but tends to be connected at grain boundaries. Figure 5 and Figure 6 shows the microstructure of Al and Al-1%HEA in the as-cast condition. It can be seen that the eutectic HEA powder is not uniformly distributed and most of it is accumulated at the grain boundaries.

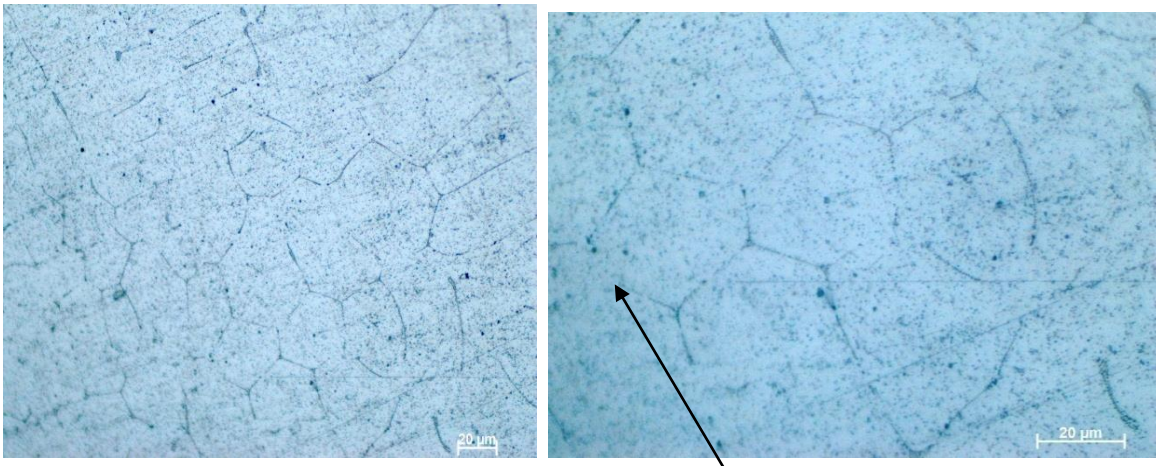

Fig 14 – Microstructure of Al observed on optical microscope at (a) 50x and (b) 100x

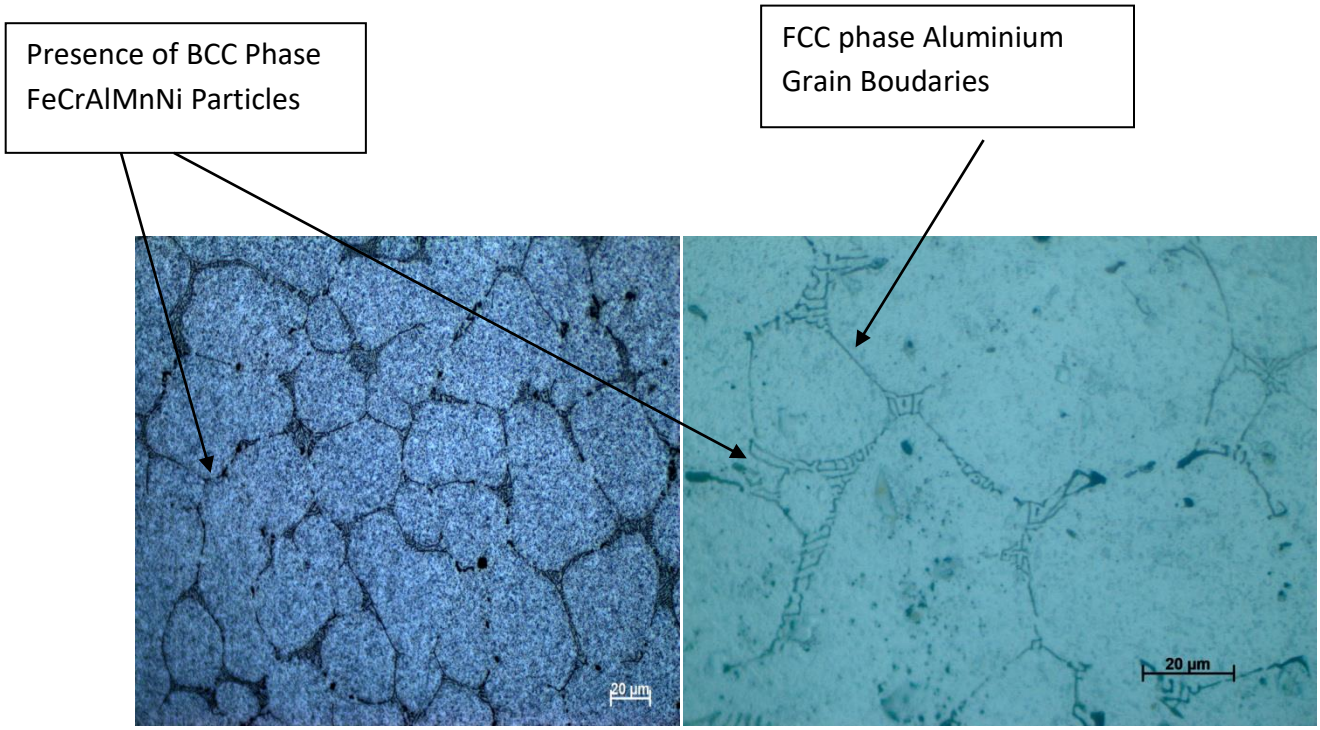

Fig 15 – Microstructure of Al – 1% HEA at (a) 50x and (b) 100x

Relatively uniform distribution was observed in almost all the composites produced. However, there are some particle-free zones due to particle pushing effects during solidification and some particle agglomeration[34]. In can also be seen that the aluminium grain structure is equiaxed in shape. This is attributed to the effect of stirring action in the semi-solid condition. This stirring action breaks the dendrite shaped structure and leaves the structure in equiaxed form[34].Another importance of this microstructure study was to determine the effect of temperature gradient on microstructure as heat during cooling of cast product flows from center of cylindrical mould (800°C) to the wall of the mold (Room temperature) and may affect

the microstructure at different distance from center[35]. Hence, in each of specimen, area was divided into 7 parts (fig. 7) and microstructures on each region have been reported in fig. 8,9.

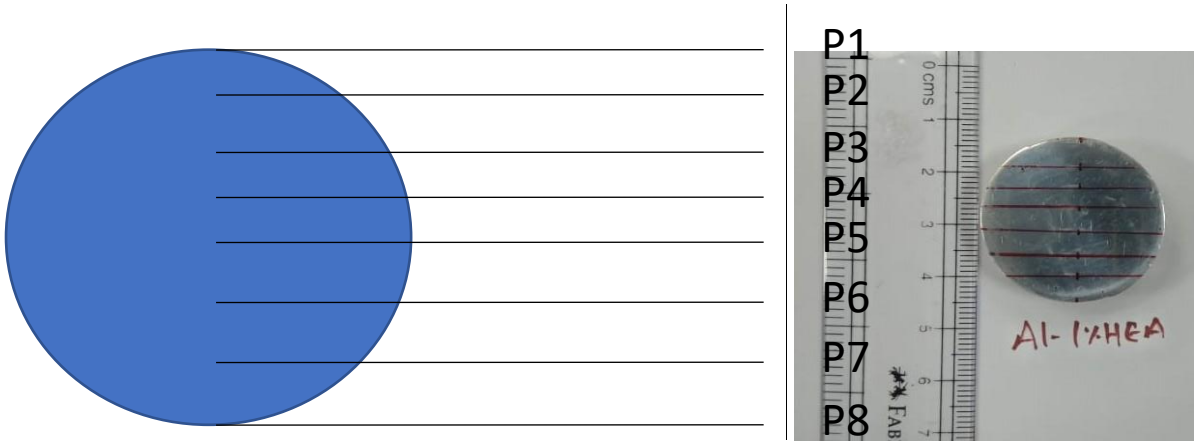

Fig.16 – Naming of points for marking different areas on the specimen and original specimen.

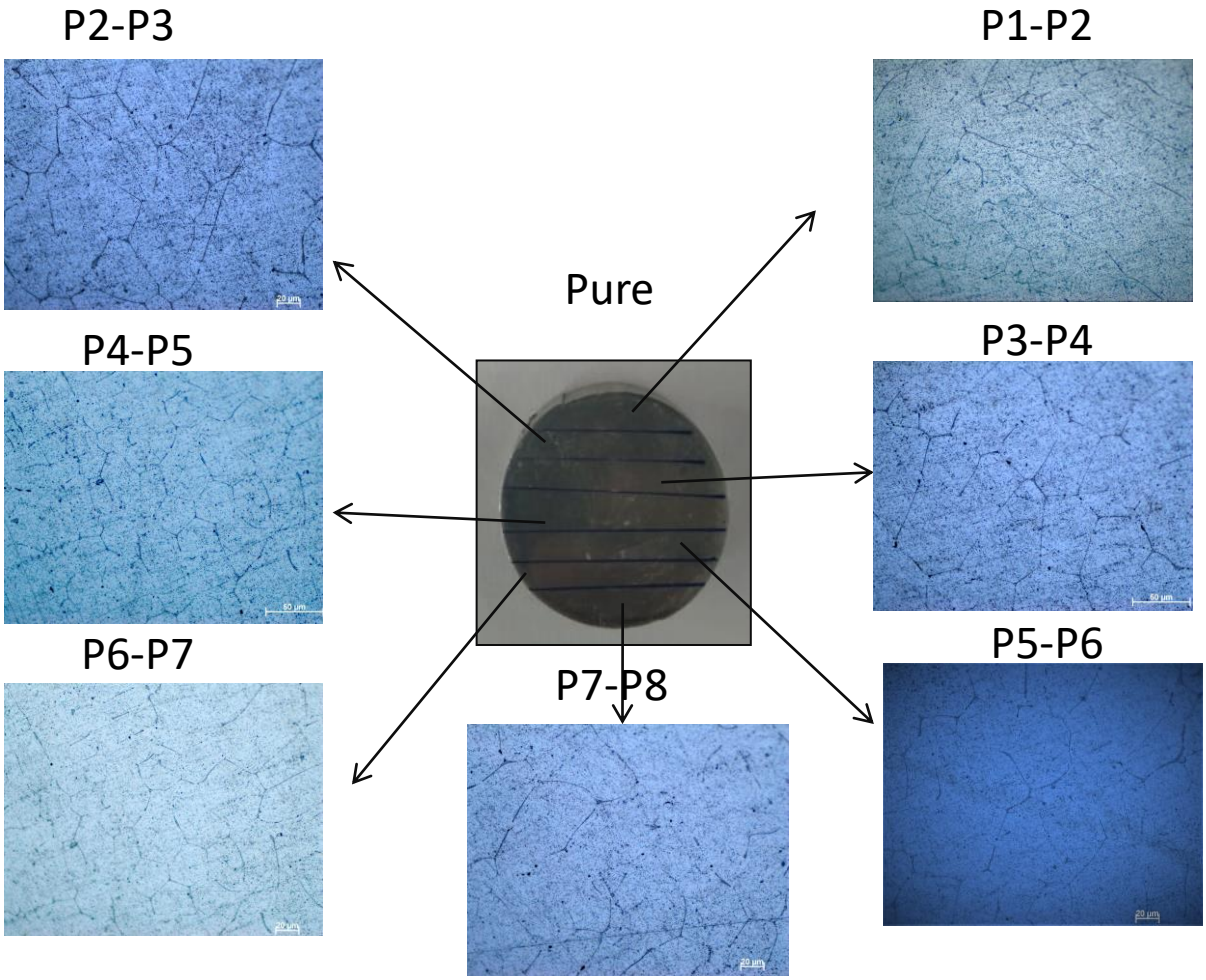

Figure 17 – As cast microstructure in 7 areas of pure Al

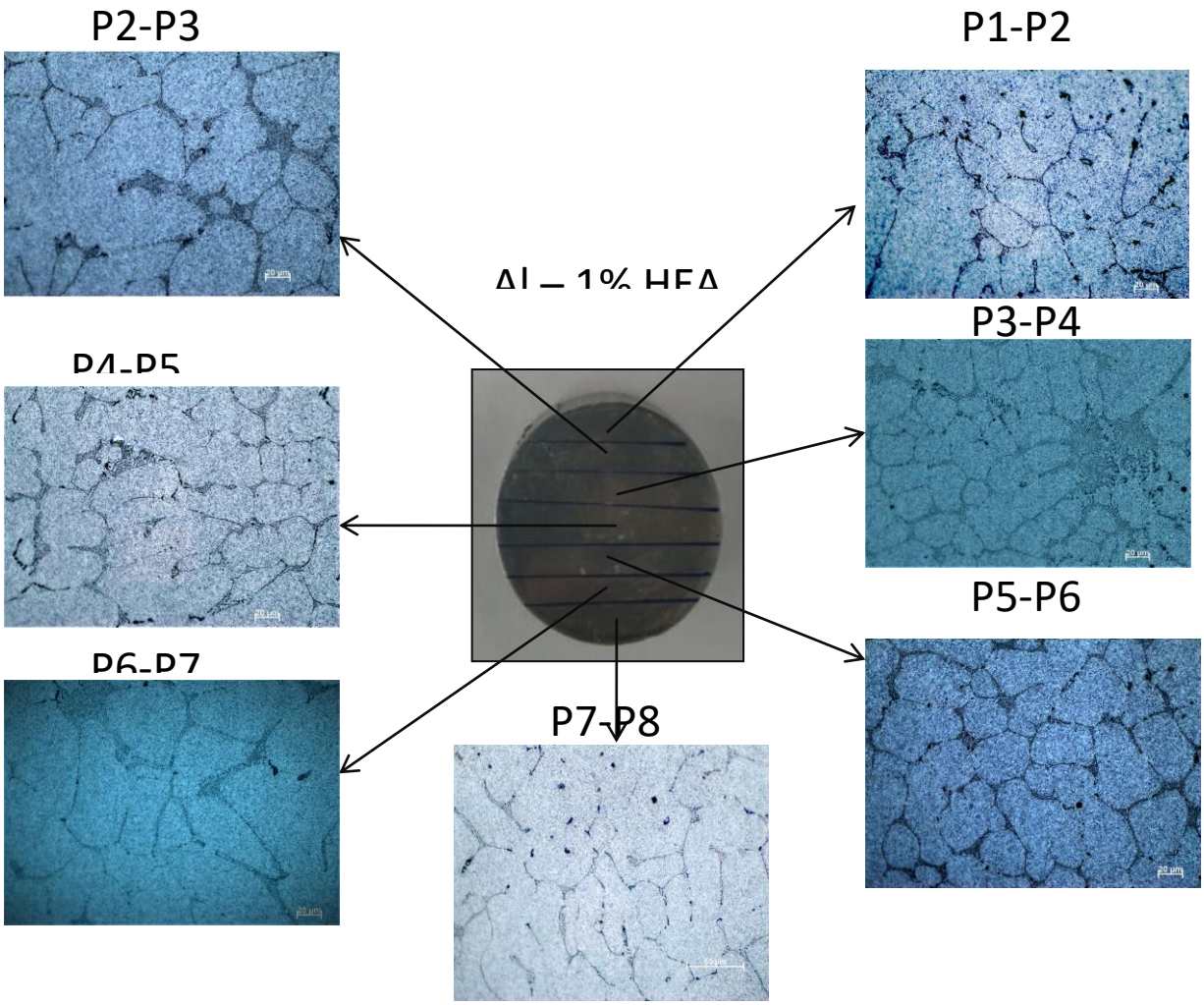

Fig 18 – As cast microstructure of Al-1% HEA

From the above microstructure profile along the radial direction, no significant change in microstructure is observed along the radial direction which indicates homogenous particle distribution during casting. This is possibly because cooling was done slowly in atmosphere for 3 hrs and hence, no significant change is observed by cooling effect during solidification.

4.2.2 Mechanical Properties analysis of sample :-

Hardness values for pure Al specimen and three specimens of Al-1% HEA at three different portions of cast ingot is reported in table 1.As shown in fig. 8 three indentations were made on each specimen in radial direction at centre, 5mm from center, and 10mm from center and hardness profile on each sample is reported.

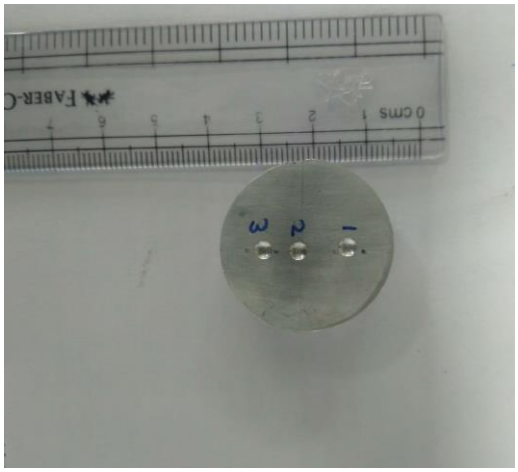

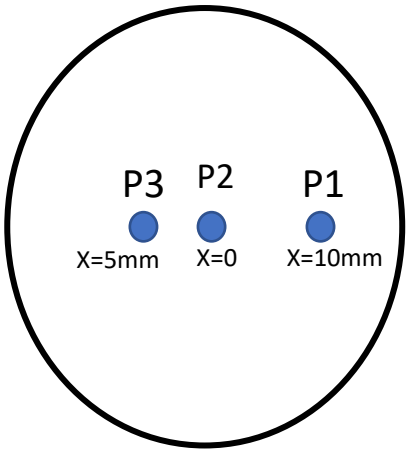

Fig. 19 : 5mm Indentations by brinell tester at different distance from centre

Specimen (as cast)	P1(HB)	P2(HB)	P3(HB)	Avg.(HB)
Pure Al	64.71	65.61	62.16	64.17
Al-1%HEA (Top)	86.61	85.71	90.09	87.45±2.31
Al-1%HEA (Middle)	88.83	91.26	87.72	89.28±1.80
Al-1%HEA (Bottom)	84.75	90.63	87.18	63.51±2.94

Table 4: hardness values of Al-HEA composites at different distance from centre

Above experimental data shows hardness of pure al (64.17 HB) and Al-1% HEA (Avg = 88.08 HB).

Hence, there is increase of 37.26% is observed in hardness of Pure Al. The increase in hardness is attributed to the FeCrAlMnNi HEA reinforcement as the reinforcement is harder and well bonded to the aluminium matrix which prevents the movement of dislocations and thus increasing hardness of composites.

Theoretically, the hardness of cast ingot should be uniform from top to bottom of the ingot. However, other factors like gravity effect, cooling effect during solidification can disturb the uniformity of distribution and may lead to different values of hardness in different regions. The above experimental data shows that the hardness is maximum at centre as compared to top and bottom parts of ingot. This indicates the higher concentration of HEA particles in middle portion of the ingot which is possibly due to the reason that the solidification starts from bottom as according to the pouring method first drop of melt settles to the bottom and

solidifies and thus prevents the settling of other reinforcement particles. Sedimentation of reinforcement particles takes place in upper region and hence the concentration becomes low in upper region. The settlement of reinforcement particles takes place in middle part of the ingot. Which results in maximum hardness at centre of ingot[34].

4.3 Analysis of samples prepared by Powder metallurgy Route

4.3.1 SEM Images of Composite Prepared by Ball Milling

SEM images of different compositions of Al reinforced with HEA are shown below :-

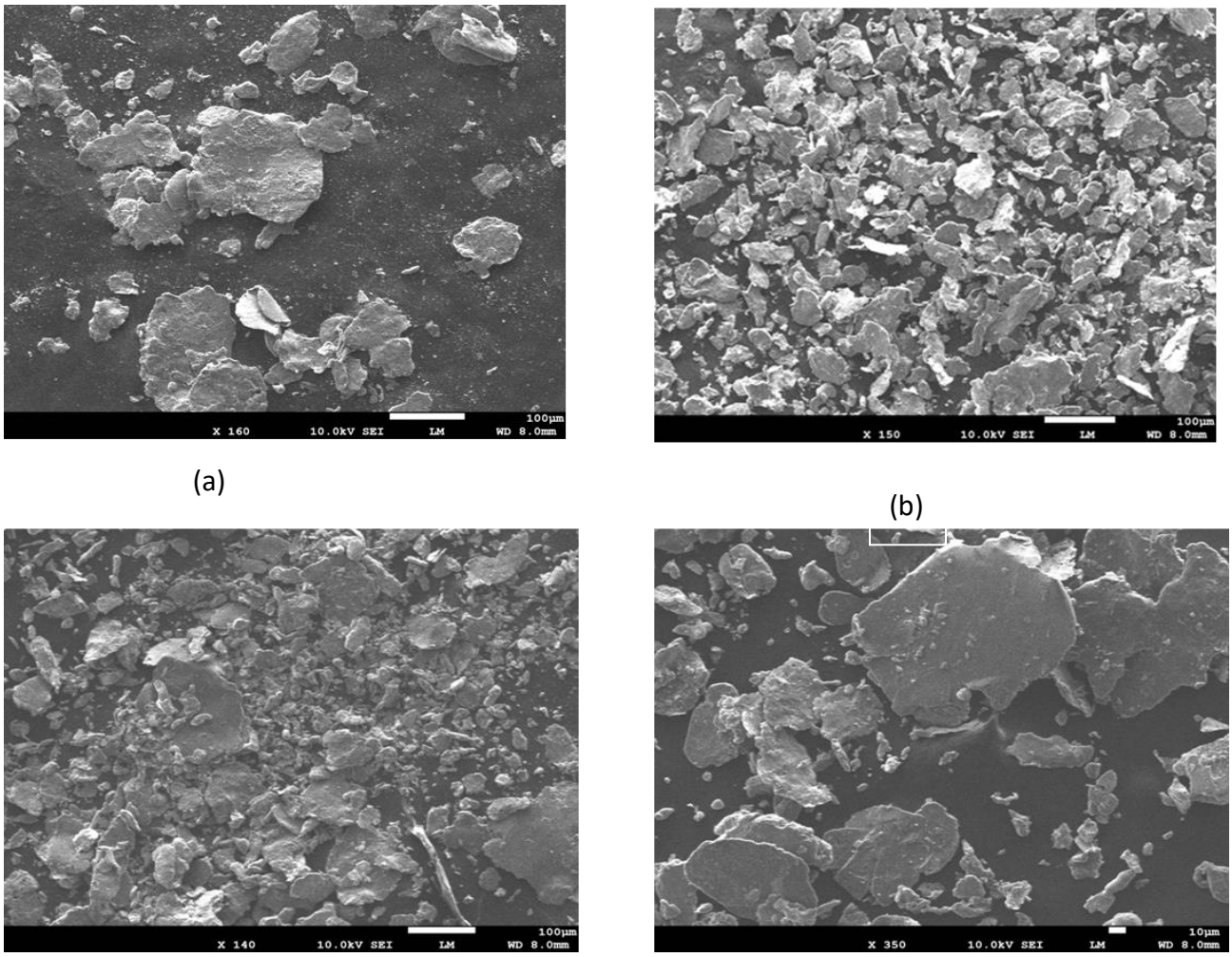

Fig. 20 – SEM images of (a) Pure Al (b) Al -1% HEA (c) Al – 5%HEA (d) Al – 10%HEA

4.3.2 X-Ray Diffraction Analysis

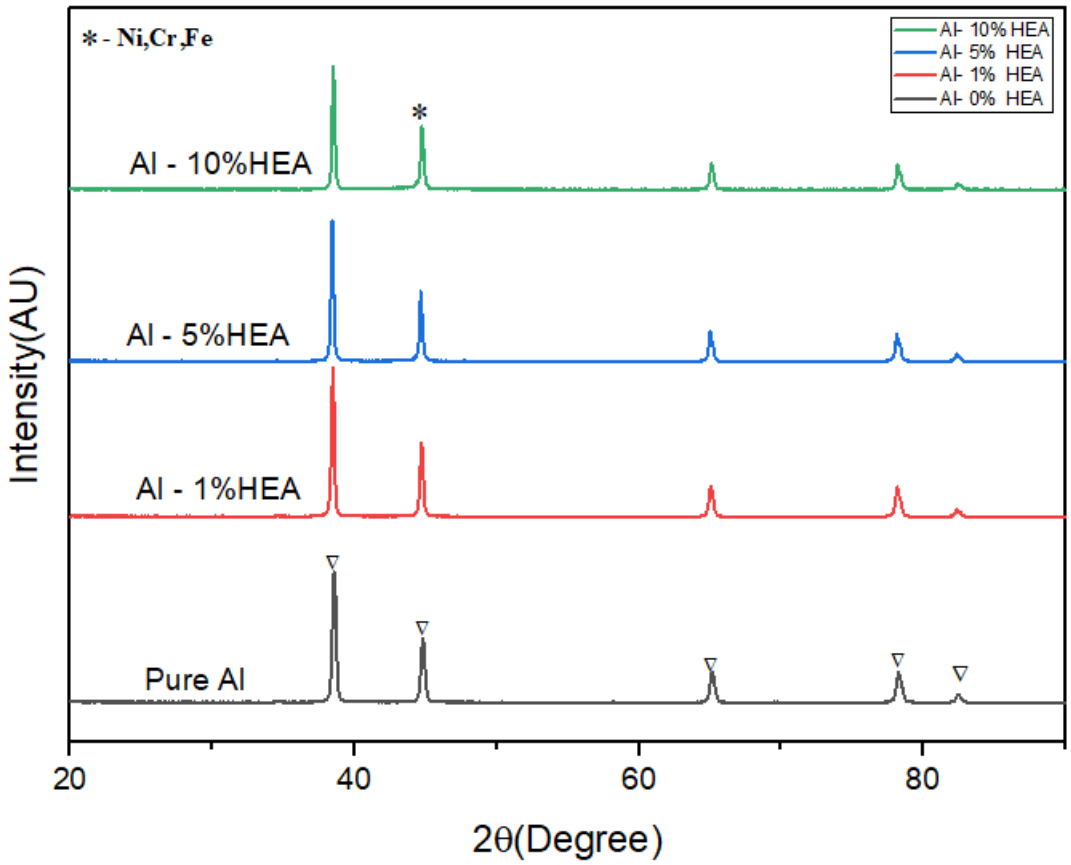

Fig. 21 – XRD of Al-HEA powder with different HEA content

XRD of 4 composites samples is shown. There is not any peaks belonging to the other phases which prove no presence of destructive chemical reactions between phases.

4.3.3 Microstructure Analysis of samples

Microstructure at different scales reveals that the dark spots shows porosity in the sample. Light coloured part is Aluminium matrix and grey part in the microstructure shows the presence of FeCrAlMnNi High Entropy Alloy particles present between the Al matrix.

The predictions were further confirmed by EDS microscopy of SEM images, discussed in next section.

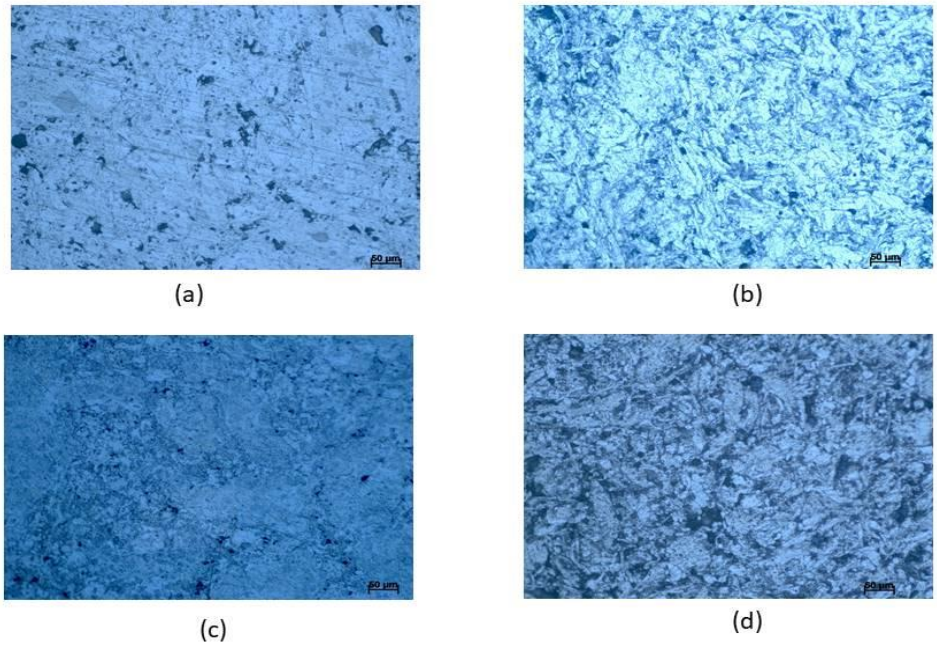

Fig.22 – Microstructure of (a) Pure-Al (b) Al – 1%HEA (c) Al – 5% HEA (d) Al – 10%HEA by optical microscope at 20x observed by optical microscope

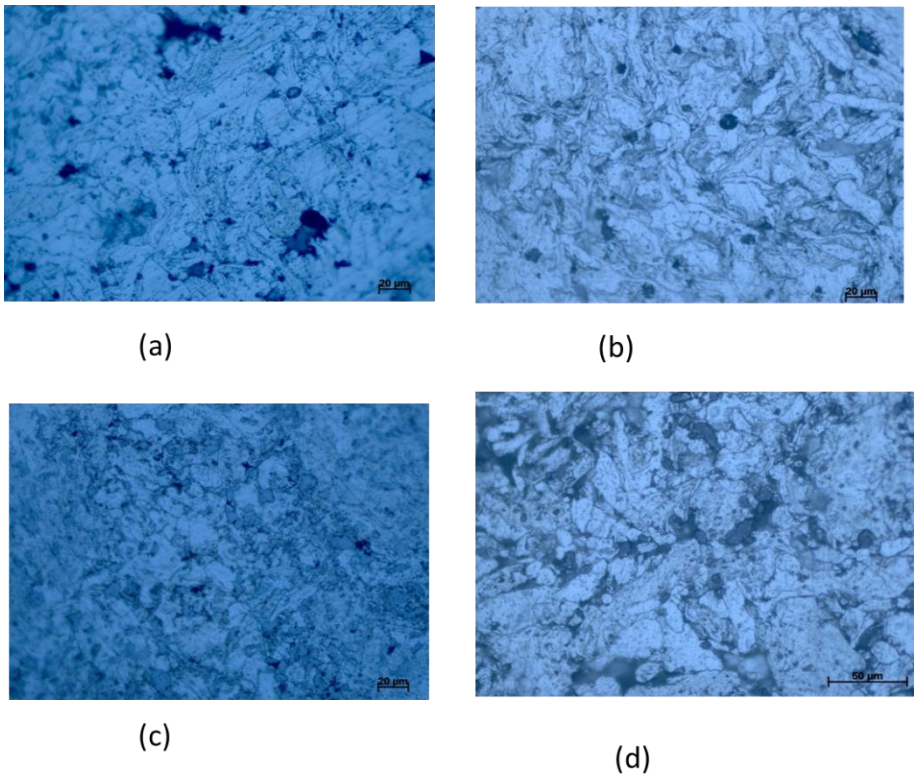

Fig. 23 – Microstructure of (a)Pure Al (b) Al – 1%HEA (c) Al – 5%HEA (d) Al – 10%HEA at 50x observed by optical microscope

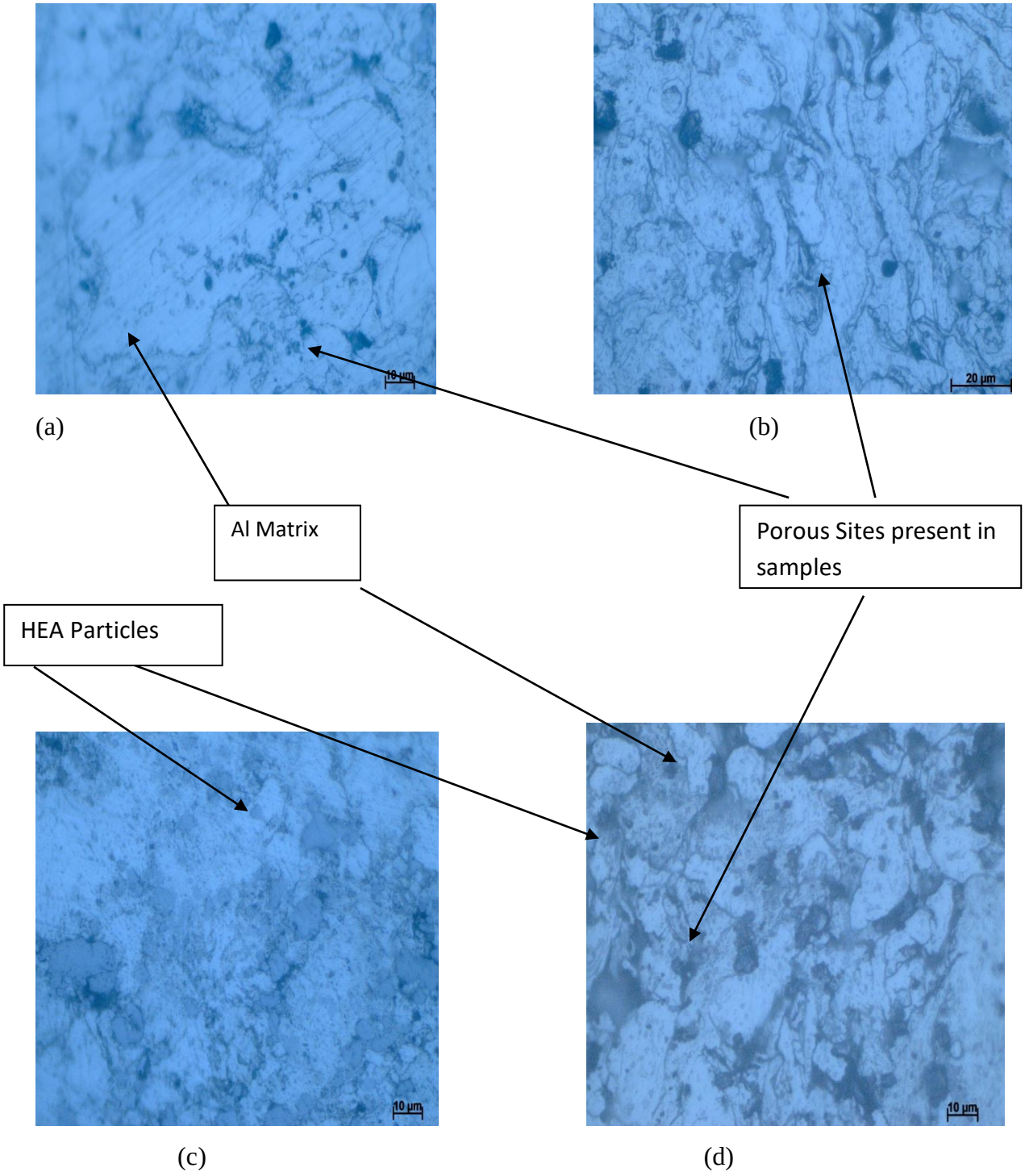

Fig. 24 – Microstructure of (a) Pure Al (b) Al – 1%HEA (c) Al – 5%HEA (d) Al – 10%HEA at 100x observed by optical microscope

4.3.4 EDS Analysis

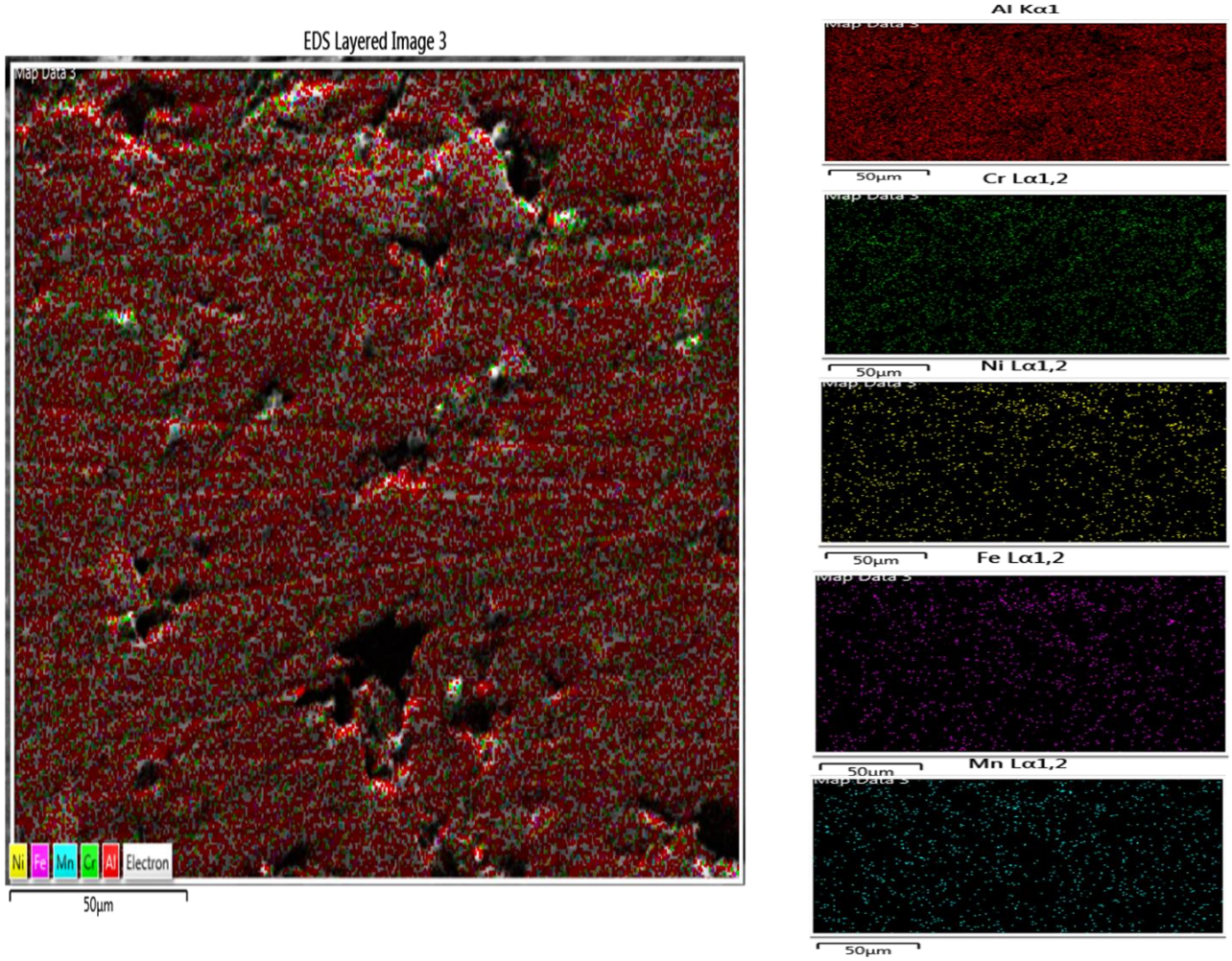

Figure 25 (a): EDS mapping of Al - 1%HEA

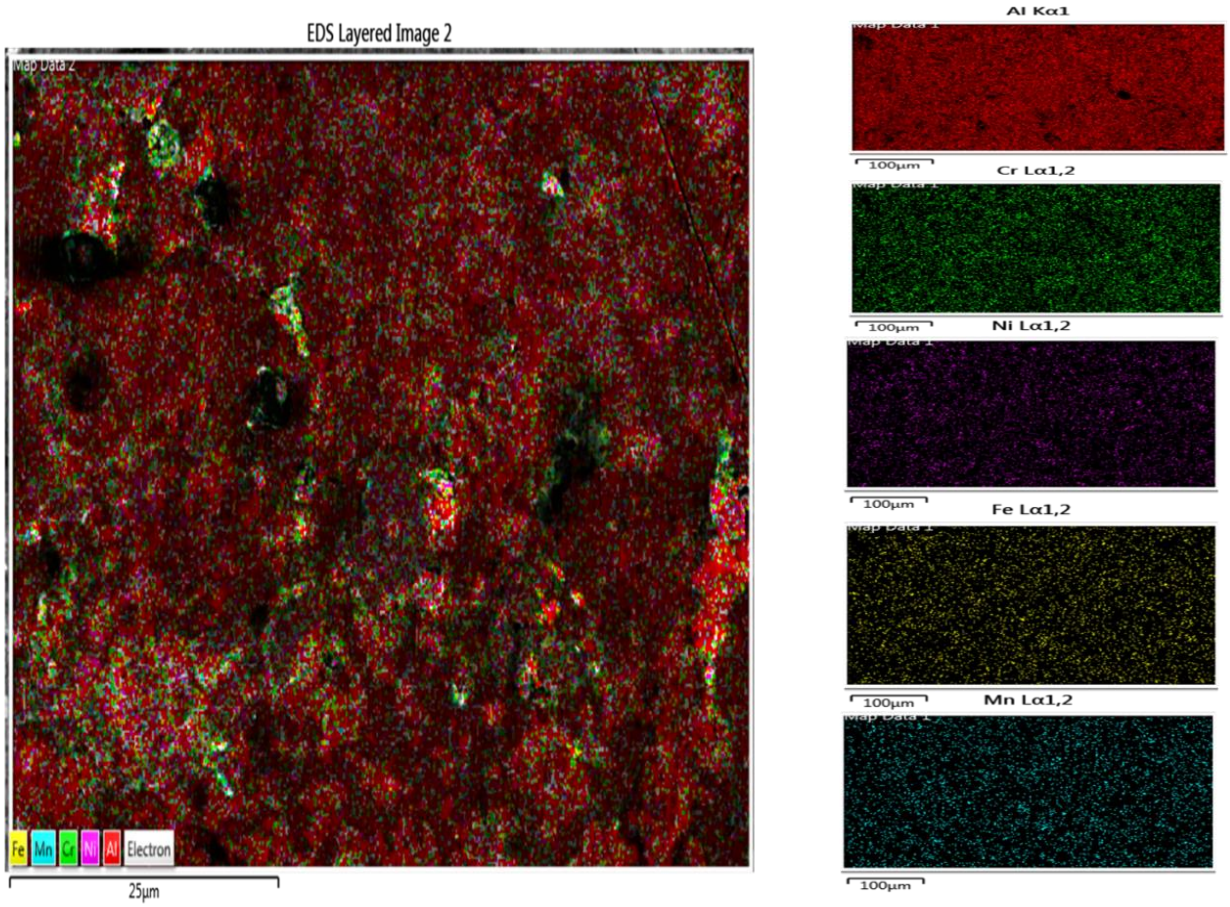

Fig. 26 – EDS mapping of Al – 5%HEA

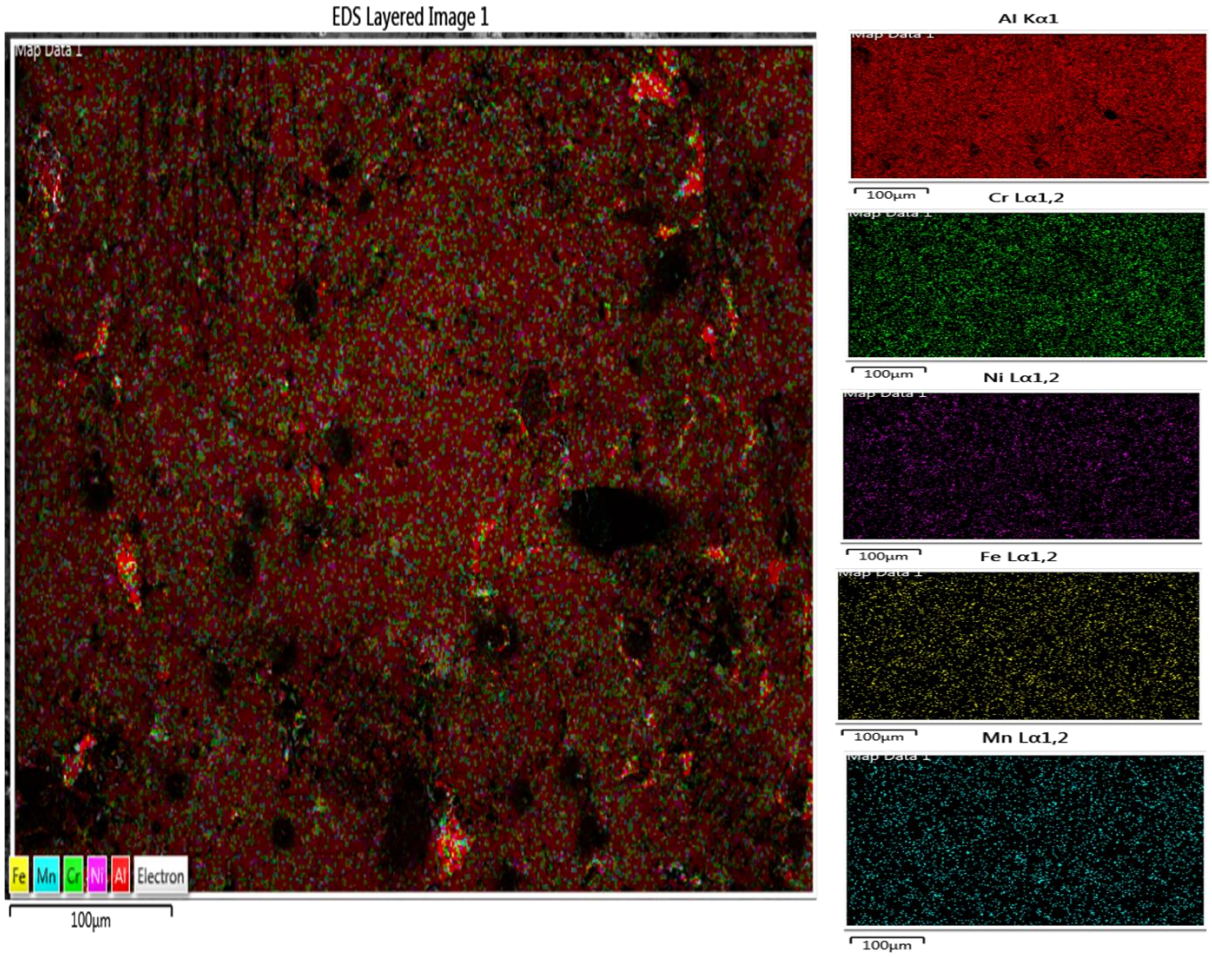

Fig. 27 – EDS mapping of Al – 10%HEA

EDS mapping shows that the reinforcement particles are distributed uniformly throughout the surface, present between the Aluminium Matrix.

4.3.5 Mechanical Properties Analysis

Brinell Hardness Test

Specimen(as cast)	Brinell Hardness(HB)
Pure Al	36.99
Al-1%HEA	52.14
Al-5%HEA	41.61
Al-10%HEA	39.03

Table 5 – Hardness value of Al-HEA composites

Comparison of the hardness of pure Al sample sintered composites proved that addition of FeCrAlMnNi boosts hardness of pure Al samples. This can be attributed to the harder HEA

particles compared to the Al and also its role in enhancement of the density of dislocations and prohibiting of Al grain growth [36].

However, the hardness is decreased in 5% HEA and 10%HEA reinforced sample because of low effect of sintering, Al-HEA interface increases and micropores increases resulting in decreased hardness of sample[36]

Chapter 5

Summary Conclusion and Future Scope

From these results following results can be drawn:-

1. FeCrAlMnNi high entropy alloy is synthesized using high energy ball milling, and its characterization indicates formation of BCC phase after 20hr of milling.
2. Crystallite size reduces from 20.49 nm in 10 minutes to 5.279 nm in 20 hrs because of continuous impact by ball milling.
3. Microstructure of pure Al and Al-1%HEA reveals that the body centered cubic (BCC) phase HEA particles are accumulated at the grain boundaries of Face centered Cubic(FCC) phase.
4. Microstructure profile along the heat flow direction shows no significant effect of cooling during solidification of cast ingot.
5. As cast hardness of Al increased significantly on addition of 1%HEA powder which was due to strong binding of hard high entropy alloy particles to Al grain boundaries.
6. Hardness was found maximum in center of ingot due to the mechanism involved in pouring of melt into the mould.
7. Hardness is more in Stir Casting sample than powder metallurgy sample.
8. Hardness boosts after reinforcing FeCrAlMnNi High Entropy Alloy in Al matrix.
9. In powder metallurgy route increased concentration of reinforcement can lead to decreased hardness, due to low effects of sintering.
10. Low effects of sintering leads to increased porosity and increased Al-HEA interface, which is found responsible for decreased hardness.

- **Future Scope of the project:-**

1. In stir casting samples with more concentration of HEA can be explored.
2. Concentration at which composite with powder metallurgy route provides maximum hardness can be worked out.
3. Heating effects on composite can be found out using different sintering temperatures in both stir casted products and powder metallurgy.

Thus, composites with different strength, densities, and thermal stabilities can be synthesized.

References:-

[1] I. Carcea, R. Chelariu, L. Asavei, N. Cimpoeşu, and R. M. Florea, "Investigations on composites reinforced with HEA particles," *IOP Conf. Ser. Mater. Sci. Eng.*, vol. 227, no. 1, 2017.

[2] K. U. Kainer, *Basics of Metal Matrix Composites*. 2006.

[3] M. C. G. J. Yeh, P. K. Liaw, and Y. Zhang, "High-Entropy Alloys."

[4] D. K. Koli, "Properties and characterization of Al-Al 2 O 3 composites processed by casting and powder metallurgy routes (review)," *nternational J. Latest Trends Eng. Technol.*, vol. 2, no. 4, pp. 486–496, 2013.

[5] Y. Li, Q. Li, D. LI, W. Liu, and G. SHU, "Fabrication and characterization of stir casting AA6061—31%B4C composite," *Trans. Nonferrous Met. Soc. China*, vol. 26, Sep. 2016.

[6] B. S. Murty, J. W. Yeh, and S. Ranganathan, "Chapter 2 - High-Entropy Alloys: Basic Concepts," B. S. Murty, J. W. Yeh, and S. B. T.-H. E. A. Ranganathan, Eds. Boston: Butterworth-Heinemann, 2014, pp. 13–35.

[7] W. Chen *et al.*, "Effect of ball milling on microstructure and mechanical properties of 6061Al matrix composites reinforced with high-entropy alloy particles," *Mater. Sci. Eng. A*, vol. 762, no. June, p. 138116, 2019.

[8] S. Raygan, H. Abdizadeh, and A. E. Rizi, "Evaluation of Four Coals for Blast Furnace Pulverized Coal Injection," *J. Iron Steel Res. Int.*, vol. 17, no. 3, pp. 8-12,20, 2010.

[9] S. J. Mary, R. Nagalakshmi, and R. Epshiba, "High Entropy Alloys Properties and Its Applications – an Overview," *High entropy Alloy. Sect. B-Review Eur. Chem. Bull*, vol. 4, no. 6, pp. 279–284, 2015.

[10] A. Pal, A. Verma, B. C. Kandpal, and sansar saxsena, "Stir Casting of Metal Matrix Composites – A Review," *Int. J. Comput. Math. Sci.*, vol. ISSN 2347, pp. 2347–8527, Mar. 2015.

[11] W. B. James and H. Corporation, "Powder Metallurgy Methods and Applications," *Powder Metall.*, vol. 7, pp. 9–19, 2018.

[12] A. M. K. Esawi, K. Morsi, A. Sayed, M. Taher, and S. Lanka, "Effect of carbon nanotube (CNT) content on the mechanical properties of CNT-reinforced aluminium composites," *Compos. Sci. Technol.*, vol. 70, no. 16, pp. 2237–2241, 2010.

[13] S. G. Kulkarni, J. V. Meghnani, and A. Lal, "Effect of Fly Ash Hybrid Reinforcement on Mechanical Property and Density of Aluminium 356 Alloy," *Procedia Mater. Sci.*, vol. 5, pp. 746–754, 2014.

[14] M. O. Bodunrin, K. K. Alaneme, and L. H. Chown, "Aluminium matrix

hybrid composites: A review of reinforcement philosophies; Mechanical, corrosion and tribological characteristics," *J. Mater. Res. Technol.*, vol. 4, no. 4, pp. 434–445, 2015.

[15] J. Chen *et al.*, "Fabrication and mechanical properties of AlCoNiCrFe high-entropy alloy particle reinforced Cu matrix composites," *J. Alloys Compd.*, vol. 649, pp. 630–634, 2015.

[16] A. Munitz, L. Meshi, and M. J. Kaufman, "Heat treatments' effects on the microstructure and mechanical properties of an equiatomic Al-Cr-Fe-Mn-Ni high entropy alloy," *Mater. Sci. Eng. A*, vol. 689, no. January, pp. 384–394, 2017.

[17] S. Natarajan, R. Narayanasamy, S. P. Kumaresh Babu, G. Dinesh, B. Anil Kumar, and K. Sivaprasad, "Sliding wear behaviour of Al 6063/TiB2 in situ composites at elevated temperatures," *Mater. Des.*, vol. 30, no. 7, pp. 2521–2531, 2009.

[18] T. V. Christy, N. Murugan, and S. Kumar, "A Comparative Study on the Microstructures and Mechanical Properties of Al 6061 Alloy and the MMC Al 6061/TiB₂/12_p," *J. Miner. Mater. Charact. Eng.*, vol. 09, no. 01, pp. 57–65, 2010.

[19] P. Li, Y. Li, Y. Wu, G. Ma, and X. Liu, "Distribution of TiB2 particles and its effect on the mechanical properties of A390 alloy," *Mater. Sci. Eng. A*, vol. 546, pp. 146–152, Mar. 2014.

[20] H. B. Rajan, R. Sundaresan, I. Dinaharan, and V. Santhiyagu, "Synthesis and characterization of in situ formed titanium dioride particulate reinforced AA7075 aluminum alloy cast composites," *Mater. Des.*, vol. 44, pp. 438–445, Feb. 2013.

[21] S. Suresh, N. Shenbaga Vinayaga Moorthi, S. C. Vettivel, N. Selvakumar, and G. Jinu, "Effect of graphite addition on mechanical behavior of Al6061/TiB2 hybrid composite using acoustic emission," *Mater. Sci. Eng. A*, vol. 612, pp. 16–27, Aug. 2014.

[22] J. James, K. Venkatesan, P. Kuppan, and R. Radhakrishnan, "Hybrid Aluminium Metal Matrix Composite Reinforced with SiC and TiB2," *Procedia Eng.*, vol. 97, Dec. 2014.

[23] M. Karbalaei Akbari, H. R. Baharvandi, and K. Shirvanimoghaddam, "Tensile and fracture behavior of nano/micro TiB2 particle reinforced casting A356 aluminum alloy composites," *Mater. Des.*, vol. 66, no. PA, pp. 150–161, 2015.

[24] Q. Gao, S. Wu, S. Lü, X. Duan, and Z. Zhong, "Preparation of in-situ TiB2 and Mg2Si hybrid particulates reinforced Al-matrix composites," *J. Alloys Compd.*, vol. 651, pp. 521–527, Dec. 2015.

[25] J. B. Fogagnolo, E. M. Ruiz-Navas, M. H. Robert, and J. M. Torralba, "The effects of mechanical alloying on the compressibility of aluminium matrix composite powder," *Mater. Sci. Eng. A*, vol. 355, no. 1–2, pp. 50–55, 2003.

[26] E. R. Chevvakula, Y. K. P, S. Sivananthan, and D. Vijayaganapathy, “INVESTIGATION OF MECHANICAL PROPERTIES FOR Al-SiC-Ti B 2 METAL MATRIX COMPOSITE .,” vol. 118, no. 24, pp. 1–9, 2018.

[27] A. A. Bunaciu, E. gabriela Udriştioiu, and H. Y. Aboul-Enein, “X-Ray Diffraction: Instrumentation and Applications,” *Crit. Rev. Anal. Chem.*, vol. 45, no. 4, pp. 289–299, 2015.

[28] A. Billah, “Investigation of multiferroic and photocatalytic properties of Li doped BiFeO3 nanoparticles prepared by ultrasonication,” 2016.

[29] M. Eduard, I. Tiginyanu, K. Nielsch, and V. Ursaki, “Porosification of semiconductor compounds III- V and II-VI : comparative study of InAs , InP , ZnSe and ZnCdS,” no. March 2015, 2013.

[30] E. W. K. Loh, D. Wijeyesekera, and M. Ciupala, “A New Method for Estimating the Moisture Content and Flexibility of Polymerised Bentonite Clay Mat,” *J. Eng. Sci. Technol.*, vol. IN PRESS, Apr. 2017.

[31] S. Kumar, V. Kumar, and P. Sahu, “ScienceDirect Synthesis and characterization of hydrogenated novel AlCrFeMnNiW high entropy alloy,” *Int. J. Hydrogen Energy*, no. xxxx, 2019.

[32] M. Kataria and S. K. Mangal, “Characterization of aluminium metal matrix composite fabricated by gas injection bottom pouring vacuum multi-stir casting process,” *Kov. Mater.*, vol. 56, no. 4, pp. 231–243, 2018.

[33] A. L. Patterson, “The scherrer formula for X-ray particle size determination,” *Phys. Rev.*, vol. 56, no. 10, pp. 978–982, 1939.

[34] J. Hashim, “The Production of Cast Metal Matrix Composite by a Modified Stir Casting Method,” *J. Teknol.*, vol. 35, no. 1, pp. 9–20, 2001.

[35] A. Singh, Y. Osawa, H. Somekawa, and T. Mukai, “Effect of solidification cooling rate on microstructure and mechanical properties of an extruded Mg-Zn-Y alloy,” *Metals (Basel).*, vol. 8, no. 5, 2018.

[36] H. Abdizadeh, R. Ebrahimifard, and M. A. Baghchesara, “Investigation of microstructure and mechanical properties of nano MgO reinforced Al composites manufactured by stir casting and powder metallurgy methods: A comparative study,” *Compos. Part B Eng.*, vol. 56, pp. 217–221, 2014.